copy 1

DIRECT DIGITAL CONTROL ALGORITHM

FOR LOW POWER NUCLEAR REACTORS

by

G. A. Harvey

B.Sc.(Eng)(Elec) University of Pretoria 1968

A THESIS SUBMITTED IN PARTIAL FULFILMENT OF
THE REQUIREMENT FOR THE DEGREE OF
MASTER OF APPLIED SCIENCE

in the Department
of
Electrical Engineering

We accept this thesis as conforming to the
required standard

THE UNIVERSITY OF BRITISH COLUMBIA

January 1973

In presenting this thesis in partial fulfilment of the requirements for an advanced degree at the University of British Columbia, I agree that the Library shall make it freely available for reference and study. I further agree that permission for extensive copying of this thesis for scholarly purposes may be granted by the Head of my Department or by his representatives. It is understood that copying or publication of this thesis for financial gain shall not be allowed without my written permission.

Department of Electrical Engineering

The University of British Columbia
Vancouver 8, Canada

Date 15 January 1973.

ABSTRACT

A direct digital control algorithm for low power reactors is proposed using logarithmic power level as input. The logarithmic power levels allow the use of fixed point arithmic resulting in faster calculation speeds than are obtainable with algorithms using floating point arithmetic. A stability analysis for various sampled data hold types is shown to have a 25% safety margin. A time optimal control sequence for power increases is derived using switch points. The switch points are determined using simulation techniques, eliminating the use of complex and approximate calculations. A practical demand level controller is developed using machine language programming to minimize the delay from the sampling of the neutron power to the output of control action. The controller is tested with digital and analog simulations of a thermal reactor showing that a successful, near time-optimal, control algorithm with general applications to low power reactors has been developed.

TABLE OF CONTENTS

LIST OF ILLUSTRATIONS

LIST OF TABLES

NOMENCLATURE

C	Concentration of delayed neutrons (neutrons/cm^3)
E	Error between demanded neutron power and actual neutron power
E_u	Unit error (E/N)
n	Neutron density (neutrons/cm^3)
N	Neutron power level
N_d	Demanded neutron power level at present sampling
N_d'	Demanded neutron power level at next sampling
N_e	Final endpoint power level
N_f	Predicted neutron power level at next sampling if no control action from present to next sampling
N_l	Neutron power level at last sampling
N_p	Neutron power level at present sampling
N_s	Switch point power level
R_{max}	Maximum reactivity rate (mk/s)
S	Neutron source (neutrons/cm^3/sec)
T	Sample period (sec)
β	Fraction of delayed neutrons
λ	Decay constant of delayed neutrons (sec^{-1})
ℓ	Mean effective neutron lifetime (sec)
δN	Deviation of neutron density from steady state
δk	Reactivity (mk)
ϵ	Error between logarithmic demand power level and logarithmic neutron power level
τ	Reactor period (sec)
τ_e	Minimum allowable reactor period at endpoint (sec)
τ_l	Minimum allowable reactor period as imposed by linear rate constraint (sec)

τ_m Minimum allowable reactor period (sec)

τ_o Minimum allowable reactor period as imposed by time optimal control constraint (sec)

PROGRAMMING NOMENCLATURE

AC	Computer accumulator
ALPHA	Variable for merging two measuring ranges
BETA(X)	Normalized fraction of delayed neutrons in the Xth group (β_x/n)
BETAT	Normalized total fraction of delayed neutrons (β/n)
BIAS	Bias added to input signal to obtain full use of A/D range
C	Constant so that demand does not diverge too far from actual neutron power
DEAD	Error deadband
DELAY(X)	Normalized concentration of neutrons in delayed group X
DERT	Inverse reactor period at final endpoint for power decreases (T/τ'_e)
DMRT	Inverse reactor period at switch point for power decreases (T/τ'_m)
DRAT	Inverse reactor period for power decreases (T/τ_m)
EP	Endpoint (Flag)
ERRO	Error between logarithmic demand power level and logarithmic neutron power level
FLXD	Logarithmic demand power level of present sampling
FLXE	Logarithmic final endpoint power level
FLXL	Logarithmic neutron power level at last sampling
FLXP	Logarithmic neutron power level at present sampling
FLXT	Temporary storage for neutron power levels
FUNC(X)	Input function for delayed group X integration calculation
GAIN	Controller gain variable
HI	Upper end of merging range for two measuring ranges
LAMDA(X)	Decay constant of delayed group X
LIND	Linear demand power level

LINP	Linear neutron power level
LNRT	Inverse period for linear rate constraint
LOW	Lower end of merging range for two measuring ranges
MAXE	Error required to give maximum output signal
NRATE	Inverse reactor period (digital simulation)
PERD	Inverse reactor period (controller)
REACT	Total reactivity
RRATE	Reactivity rate
SCALE 1	Variable for calibration of A/D #1 sample
SCALE 2	Variable for calibration of A/D #2 sample
SWLD	Logarithmic switch point for linear range
SWSD	Logarithmic switch point for time optimal control range (power decreases)
SWST	Logarithmic switch point for time optimal control range (power increases)
TEMP 1 to 4	Temporary storage for digital simulation
TEM 1 to 3	Temporary storage for controller
UERT	Inverse reactor period at final endpoint for power increases (T/τ_e')
UMRT	Inverse reactor period at switch point for power increases (T/τ'_m)
URAT	Inverse reactor period for power increases (T/τ_m)
$\oplus$	Exclusive OR function

ACKNOWLEDGEMENT

The author wishes to express his gratitude to Professors F.K. Bowers and A. Soudack for their supervision of this research. Sincere appreciation is due to Dr. A.J.A. Roux, President, and Mr. W.K.H.A. Weidemann, Director: Instrumentation, of the South African Atomic Energy Board for making this study opportunity available. Thanks are due to the author's wife, Fiona, for her understanding and for typing the draft and also to Miss Norma Duggan for preparing the final manuscript.

1. INTRODUCTION

Until recently, the role of the digital computer in nuclear reactor systems has been that of a supervisory and data-collection nature[1,2]. Strict safety regulations resulted in conventional methods being used for reactor control due to the low reliability, slow speed and tremendous expense of early computers. Advances in computer technology have removed these objections. With reactor systems becoming larger and more complex, it is advantageous that digital computers be used in the control of nuclear reactors.

At first, computers were used only for individual tasks such as fuelling machine control and failed fuel detection[1]. For the actual control of nuclear reactors, dual computer systems have been used; one operational and the other in a "watchdog" and "backup" mode. With the addition of more duties, such as load matching, turbine control, spatial control and automatic fuelling, the size of the computers has entered the medium range. Each of these duties is normally handled by separate design groups. The co-ordination of these groups in the development of a single operating system is extremely difficult[1].

Recent developments make the use of several small minicomputers economically feasible[1]. Each computer is assigned its own specific task. An added advantage is that each design group can develop and commission its own separate system, without too much dependence on the other groups. Figure (1.1) shows a possible system of minicomputers working in a parallel mode. All the computers are linked together by a bus system as well as to the common mass storage units. Transfer of data to or from these mass storage units is processed by a single control computer to facilitate file orientated transfers without repetition of

software drivers.

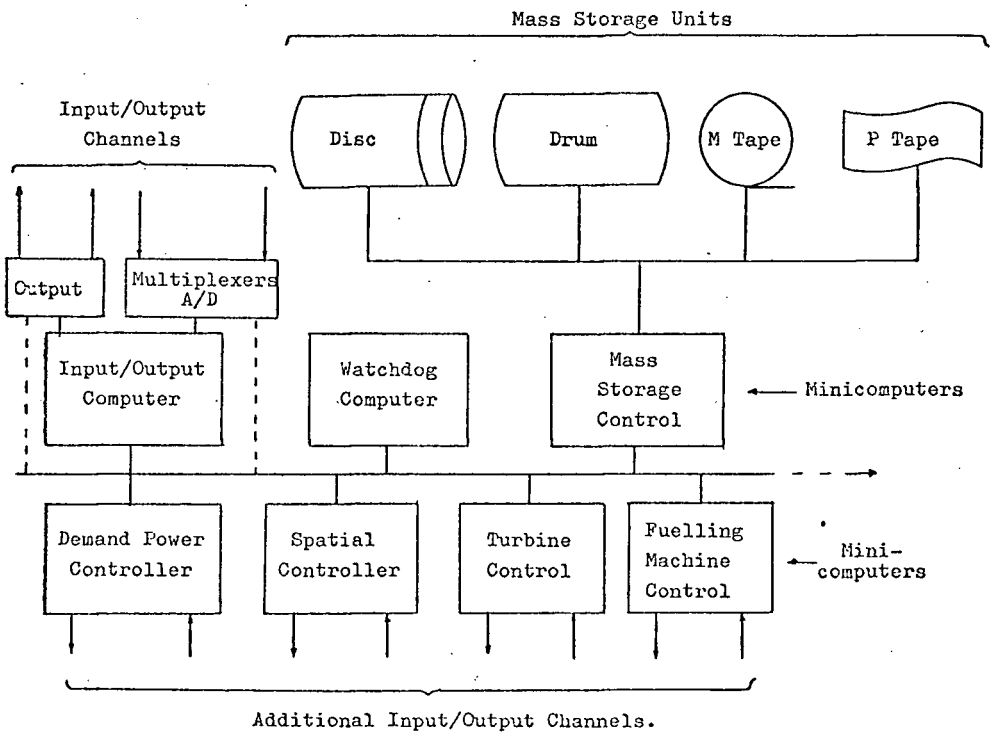

Fig. 1.1 Possible Reactor Control System Using Parallel Mode Mini-Computers.

In Chapter 2, a basic error sampled data control system is developed and the transfer functions of the various system components are given. Based on a study by Marciniak[2] the overall system stability is analysed using various sampled data holds and sample periods. A review of existing digital control algorithms is given in Chapter 3[2,3]. An algorithm requiring a logarithmic neutron power level as input is developed, resulting in a much faster and simpler digital controller. The use of logarithmic power levels allows the use of fixed point arithmetic which is much faster than floating point arithmetic. Using the results of previous studies on the time optimal control of nuclear reactors [2,4], a time optimal control sequence using switch points is developed in Chapter 4 for power level changes. The switch points are determined using simulation techniques. In Chapter 5, a practical demand power level

controller is developed using machine language programming. The performance of the controller is tested using digital and analog simulations of a thermal reactor. The stability analysis of Chapter 2 is shown to have a 25% safety margin and power level changes were effectively carried out, maintaining the reactor within the safety constraints, with little overshoot of the final end point power level.

2. DIGITAL CONTROL SYSTEMS FOR NUCLEAR REACTORS

A basic error sampled closed loop control system is presented in this section for various types of hold units. The overall system transfer functions are derived, followed by a stability analysis for low-power or zero-power reactors using a linearized point kinetics model[2].

2.1 Basic Digital Control System

A basic nuclear reactor continuous control system is shown in figure (2.1.1). The input to the system is a demand power level as well as a constraint on the minimum allowable reactor period. (The reactor period is defined as the time necessary for the power level to change by a factor "e", the natural logarithm base). These two inputs are combined with the measured reactor power level to generate an error

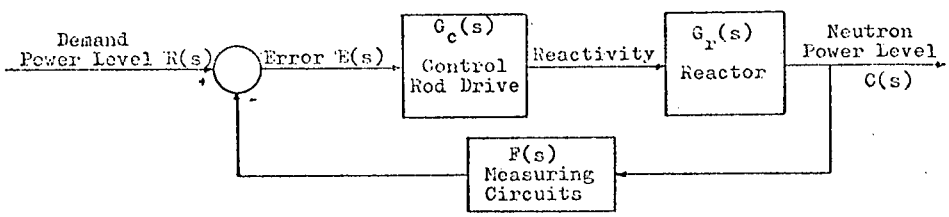

Fig. 2.1.1 Basic Block Diagram of a Continuous Reactor Control System

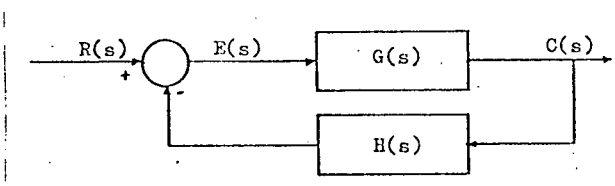

Fig. 2.1.2 General Continuous Closed Loop Control System.

signal which drives the control rods. Simplification gives the general feedback control system in figure (2.1.2) with the overall transfer function

$$\frac{C(s)}{R(s)} = \frac{G(s)}{1 + G(s)\,H(s)} \qquad (2.1.1)$$

where $G(s) = G_c(s)\, G_r(s)$ = feed-forward transfer function (2.1.2)

$H(s) = F(s)$ = feedback transfer function (2.1.3)

$G_c(s)$ = control rod transfer function (2.1.4)

$G_r(s)$ = reactor transfer function (2.1.5)

The most suitable sampled data control system to use for reactor control is the error sampled closed loop system given in figure (2.1.3). Using the z-transform notation, the overall transfer function is:

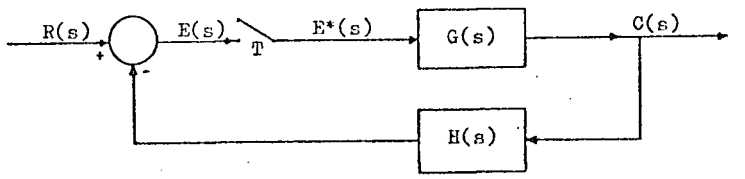

Fig. 2.1.3 General Error Sampled Closed Loop Control System

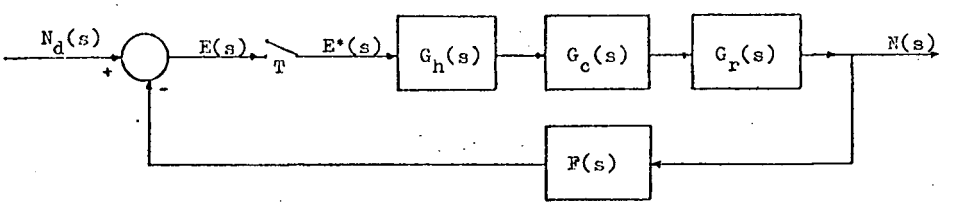

Fig. 2.1.4 Basic Sampled Data Control System for a Nuclear Reactor

$$\frac{C_z(z)}{R_z(z)} = \frac{G_z(z)}{1 + G_z H_z(z)} \qquad (2.1.6)$$

which is of similar form to that of the continuous case (see footnote). Figure (2.1.4) gives the basic sampled data control system for a reactor where $G_h(s)$ is the transfer function of the hold device following the

---

Note: Throughout this thesis the z-transform notation is the same as used in previous digital reactor control studies[2].

sampler, $G_c(s)$ the transfer function for the control rods, $G_r(s)$ the transfer function of the reactor and F(s) the transfer function of the neutron power level measuring circuits. The transfer functions of each of the system blocks will be analysed in sections 2.2 to 2.5, followed by a stability analysis of the overall system using various types of hold.

2.2 Sampled Data Holds

In the sampled data reactor control system, the sampled error is used to drive the control rods at the required velocity. A pure impulse signal is unsuitable for this task due to it being practically unrealizable and the sampled signal is passed through some hold device that performs the function of reproducing the sampled signal until the next sampling. Two basic holds are the zero order and first order holds. Holds of greater order are to be avoided, not only due to the difficulties of physical realization but also because of the delays they may introduce into the system.

2.2.1 Zero Order Hold

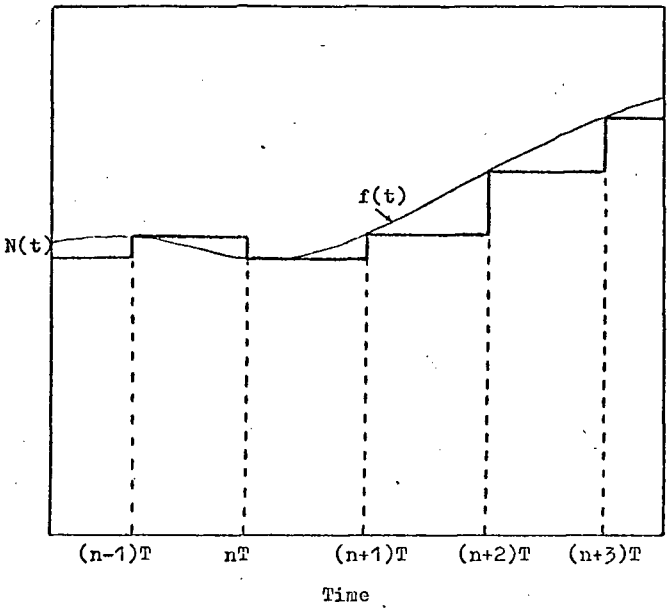

Fig. 2.2.1 Output of Zero-Order Hold Device.

If the sampled signal is held until the next sample such that

$$N(t) = f(nT) \qquad nT < t \leq (n+1)T \tag{2.2.1}$$

as in figure (2.2.1), the device is called a zero order hold and has the transfer function

$$H_o(s) = (1-\exp(-Ts))/s \tag{2.2.2}$$

In the case of the sampled data reactor control system

$$E(t) = N_d(nT) - N(nT), \; nT < t \leq (n+1)T \tag{2.2.3}$$

where N_d = demand neutron power level (reference)

N = measured neutron power level

T = sample period

E = error

2.2.2 First Order Hold

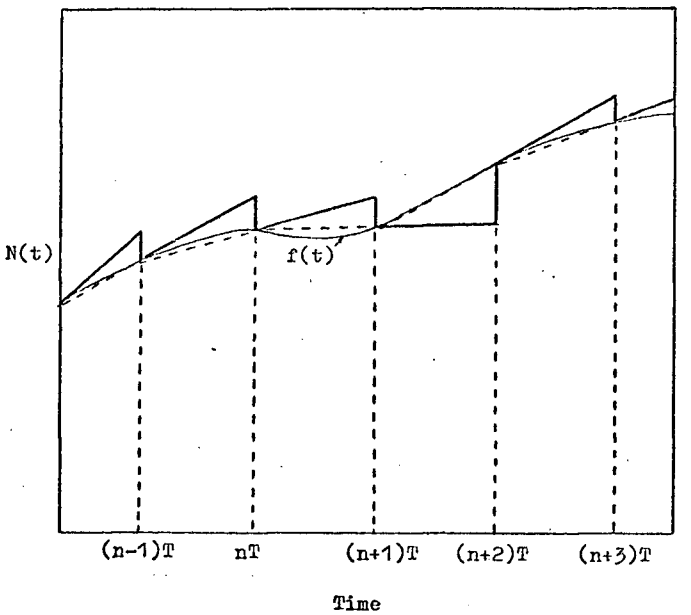

Fig. 2.2.2 Output of First-Order Hold Device

If the last two samplings are used to calculate the slope of the signal such that

$$N(t) = f(nT) + \frac{f(nT) - f[(n-1)T]}{T}(t-nT), \qquad nT < t \leq (n+1)T \tag{2.2.4}$$

as in figure (2.2.2), the device is called a first order hold and has the transfer function

$$H_1(s) = \frac{(1+Ts)}{T} \quad \frac{(1-\exp(-Ts))^2}{s} \tag{2.2.5}$$

In the case of the sampled data reactor control system

$$E(t) = E(nT) + \frac{E(nT) - E((n-1)T)}{T} (t-nT),$$

$$nT < t \leq (n+1)T \tag{2.2.6}$$

where $E(nT) = N_d(nT) - N(nT)$ (2.2.7)

and E, N_d and N are as before.

2.2.3 Linearized Hold

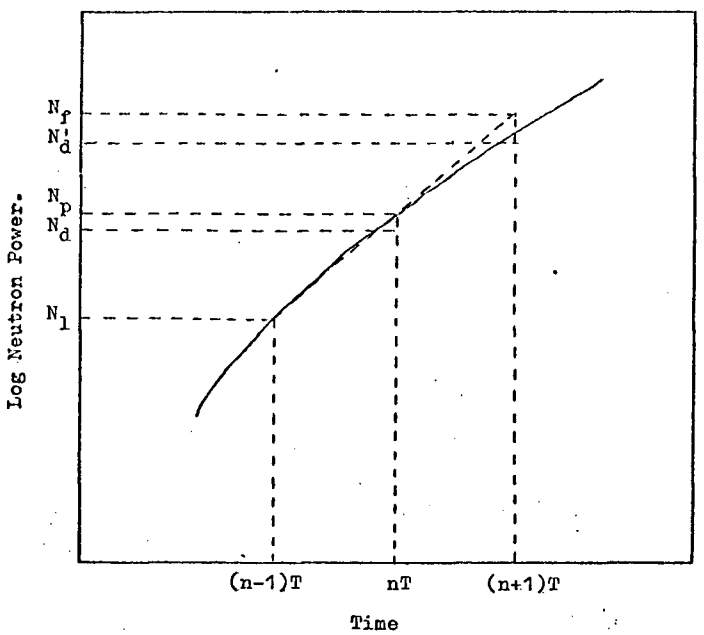

Fig. 2.2.3 Linearized Hold Device Sample Points

Cohn[3] developed a hold that has particular bearing on nuclear reactors such that

$$E'(t) = N_d[(n+1)T] - N'[(n+1)T], \quad nT < t \leq (n+1)T \tag{2.2.8}$$

where $N_d[(n+1)T] = N'_d$ = demand neutron power at next sampling

and $N'[(n+1)T] = N_f$ = predicted neutron power at next sampling if no control action is taken from the present to the next sampling.

Let $N_1 = N[(n-1)T]$ = neutron power level at last sampling

$N_p = N[nT]$ = neutron power level at present sampling

and τ_a = acutal reactor period. (See figure 2.2.3).

Now $$N_f = N_p \exp (T/\tau_a) \tag{2.2.9}$$

where the reactor period τ_a, is the inverse of the logarithmic slope of the neutron power level such that

$$1/\tau_a = (\ln N_p - \ln N_1)/T \tag{2.2.10}$$

Therefore $$N_f = N_p \exp [T(\ln N_p - \ln N_1)/T] \tag{2.2.11}$$

$$= N_p^2/N_1 \tag{2.2.12}$$

and $$E'(t) = N'_d - (N_p^2/N_1), \quad nT < t \leq (n+1)T \tag{2.2.13}$$

The transfer function of this hold can be obtained in the following manner:

Assuming that N_p and N_1 deviate only slightly from the demand N'_d and that t is the present time and T the sample period,

$$N_p = N(t) = N'_d (1+Y_p), \quad |Y_p| << 1 \tag{2.2.14}$$

and $$N_1 = N(t-T) = N'_d (1+Y_1), \quad |Y_1| << 1 \tag{2.2.15}$$

Substitution into equation (2.2.13) and neglecting high order terms of Y_p and Y_1 gives

$$E'(t) = [2Y_p - Y_1]N'_d \tag{2.2.16}$$

But from equations (2.2.14) and (2.2.15)

$$Y_p = (N(t) - N'_d)/N'_d \tag{2.2.17}$$

and $$Y_1 = (N(t-T) - N'_d)/N'_d \tag{2.2.18}$$

therefore $$E'(t) = 2[N(t) - N'_d] - [N(t-T) - N'_d] \tag{2.2.19}$$

As $$E(t) = N(t) - N'_d \ , \tag{2.2.20}$$

therefore $$E(t-T) = N(t-T) - N'_d \tag{2.2.21}$$

and $$E'(t) = 2E(t) - E(t-T) \qquad (2.2.22)$$

As the output of an error sampler is given by

$$E^*(t) = \sum_{n=0}^{\infty} E(t)\ \delta[t-nT] \qquad (2.2.23)$$

and substituting for equation (2.2.22) and taking the Laplace transform gives

$$E'^*(s) = 2E(0)\ \frac{(1-\exp(-Ts))}{s} + [2E(T) - E(0)]\ \exp(-Ts)$$

$$\frac{(1-\exp(-Ts))}{s} + [2E(2T) - E(T)]\ \exp(-2Ts)$$

$$\frac{(1-\exp(-Ts))}{s} + \ldots\ldots\ldots\ldots\ldots \qquad (2.2.24)$$

which may be simplified to

$$E'^*(s) = \frac{1-\exp(-Ts)}{s}\ [2 - \exp(-Ts)]\ E^*(s) \qquad (2.2.25)$$

Thus the transfer function of the linearized hold is

$$H_1(s) = [2-\exp(-Ts)]\ \frac{1-\exp(-Ts)}{s} \qquad (2.2.26)$$

The transfer functions for the three types of hold will be used in the overall system stability analysis to determine which hold gives the best performance.

2.3 Control Rod Servo System

The simplest transfer function for the control rod servo system is

$$G_c(s) = R/s \qquad (2.3.1)$$

where R is the reactivity rate per unit error input. A time constant should also be included in the transfer function, however, due to the complexity of the overall system gain, it is neglected. In practice, there is also a limit placed on the maximum reactivity rate which

constrains the maximum system gain. This too will be ignored[2].

2.4 Reactor Model

Examination of the differential equations for the reactor kinetics shows a reactor to be highly non-linear. (See Appendix A). Schultz[5] developed a linearized transfer function of a reactor model about a steady state power level, incorporating all six groups of delayed neutrons. Marciniak[2] and Lipinsky[4] have derived a time independent, linear, monoenergetic, one-delayed-neutron-group kinetics transfer function given as follows:

$$G_r(s) = \frac{\delta N(s)}{N_o \delta k(s)} = \frac{s + \lambda}{\ell s[s + \lambda + \beta/\ell]} \qquad (2.4.1)$$

where λ = average decay constant

β = total effective delayed neutron fraction

ℓ = prompt neutron lifetime

N_o = neutron density about which the system is linear

δk = effective reactivity

δN = deviation of neutron density from N_o.

This transfer function will be used for the reactor model in the stability analysis given in section 2.6.

2.5 Neutron Power Level Measuring Circuits

Due to reactor noise, the input to the computer must have some smoothing. The method used on the ZPR-9 fast critical reactor at the Argonne National Laboratory is very applicable for the digital monitoring of the neutron power level[3]. An ion chamber is used to measure the neutron flux and the output of the ion chamber amplifier is used to drive a voltage-to-frequency converter. The output of the voltage-to-frequency converter is fed into a counter or scaler which is read and then reset every T seconds. The counter acts as an integrator

smoothing the input to the computer. However, in most systems, computer inputs are multiplexed to measure other variables and not only the neutron power. In this case, the output of the ion chamber amplifier must be suitably filtered, depending on the sample period.

Taking the case of the counter, the average of a signal f(t) over a period T is

$$\bar{p}(t) = \frac{1}{T} \int_{t-T}^{t} p(t')\, dt' \qquad (2.5.1)$$

Taking the Laplace Transform gives

$$\bar{P}(s) = \frac{P(s)}{Ts} - \frac{P(s)\, \exp(-Ts)}{Ts} \qquad (2.5.2)$$

Therefore the Transfer Function is

$$F(s) = \frac{1 - \exp(-Ts)}{Ts} \qquad (2.5.3)$$

Schematic diagrams of the two possible neutron power level measuring circuits are given in figures (2.5.1) and (2.5.2).

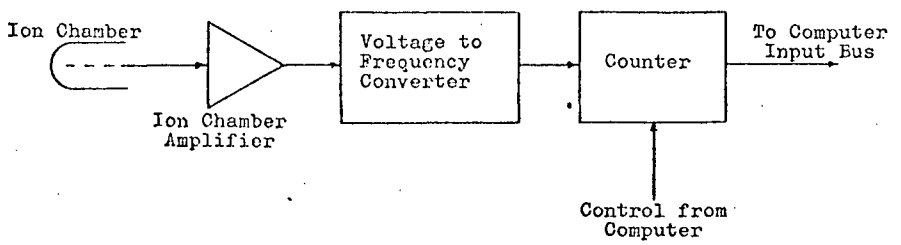

Fig. 2.5.1 Neutron Power Level Measuring Circuit Schematic (Scaler plus Voltage-to-Frequency Converter)

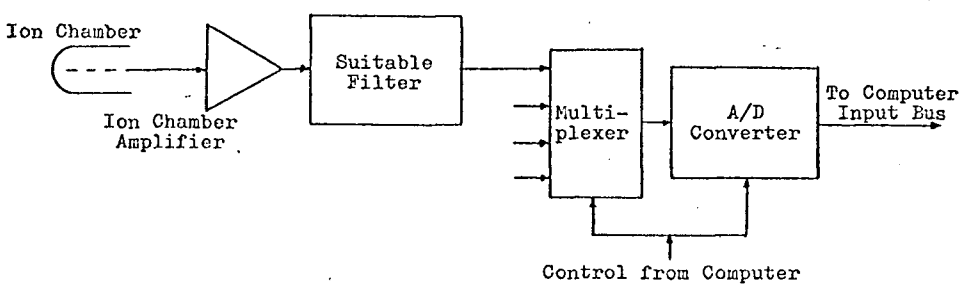

Fig. 2.5.2 Neutron Power Level Measuring Circuit Schematic (Filter plus Multiplexer plus A/D)

2.6 Overall System Stability

A basic sampled data control system for a nuclear reactor was given in figure (2.1.4) and the overall transfer function by equation (2.1.4), where

$$G_z(z) = Z[G_h(s)G_c(s)G_r(s)] \tag{2.6.1}$$

$$G_zH_z(z) = Z[G_h(s)G_c(s)G_r(s)F(s)] \tag{2.6.2}$$

and $$Z[G(s)] = G_z(z) \tag{2.6.3}$$

is the z transform of G(s).

The transfer functions for the individual system blocks have been derived in the previous sub-sections. The transfer function for the system with zero-order hold is[2]:

$$\frac{\delta N_z(z)}{N_o N_{dz}(z)} = \frac{Z[H_o(s)G_c(s)G_r(s)]}{1+Z[H_o(s)G_c(s)G_r(s)F(s)]} \tag{2.6.4}$$

$$= \frac{3\lambda' TKz(az^2+bz+c)}{6\lambda'^4 T\ell z(z-1)^2(z-\gamma)+K(dz^3+ez^2+fz+g)} \tag{2.6.5}$$

where

$$\lambda' = \lambda + (\beta/\ell) \tag{2.6.5a}$$

$$K = R/\ell \tag{2.6.5b}$$

$$\gamma = \exp(-\lambda' T) \tag{2.6.5c}$$

$$a = \lambda\lambda'^2T^2\ell+2\beta T\lambda'+2\beta(2+\gamma)-6\beta \tag{2.6.5d}$$

$$b = \lambda\lambda'^2T^2\ell(1-\gamma)-2\beta T\lambda'(1+\gamma)-2\beta(1+2\gamma)+6\beta \tag{2.6.5e}$$

$$c = -\lambda\lambda'^2T^2\ell\gamma+2\beta T\lambda'\gamma+2\beta\gamma-2\beta \tag{2.6.5f}$$

$$d = \lambda\lambda'^3T^3\ell+3\beta T^2\lambda'-6\beta T\lambda'-6\beta(3+\gamma)+24\beta \tag{2.6.5g}$$

$$e = \lambda\lambda'^3T^3\ell(4-\gamma)-3\lambda'^2T^2\beta\gamma+6\beta T\lambda'(2+\gamma)+18\beta(1+\gamma)-36\beta \tag{2.6.5h}$$

$$f = \lambda\lambda'^3T^3\ell(1-4\gamma)-3\lambda'^2T^2\beta-6\beta T\lambda'(1+2\gamma)-6\beta(1+3\gamma)+24\beta \tag{2.6.5i}$$

$$g = -\lambda\lambda'^3T^3\ell\gamma+3\lambda'^2T^2\beta\gamma+6\beta T\lambda'\gamma+6\beta\gamma-6\beta \tag{2.6.5j}$$

For the first-order hold, the transfer function is[2]:

$$\frac{\delta N_z(z)}{N_o N_{dz}(z)} = \frac{4\lambda' TK(hz^4+kz^3+mz^2+pz)}{24\lambda'^6 T^2 \ell z^2(z-1)^2(z-\gamma)+K(qz^4+rz^3+uz^2+vz+w)} \quad (2.6.6)$$

where

$$\lambda' = \lambda + (\beta/\ell) \quad (2.6.6a)$$

$$K = R/\ell \quad (2.6.6b)$$

$$\gamma = \exp(-\lambda' T) \quad (2.6.6c)$$

$$h = \lambda\lambda'^3 T^3 \ell + 3\lambda'^2 T^2(\lambda\lambda' T\ell+\beta) + 6\beta(\lambda' T-1)T + 6\beta(\lambda' T-1)(3+\gamma) - 24\beta(\lambda' T-1) \quad (2.6.6d)$$

$$k = \lambda\lambda'^3 T^3 \ell(4-\gamma) - 3\lambda'^2 T^2(\lambda\lambda' T\ell+\beta)\gamma - 6\beta(\lambda' T-1)T\lambda'(2+\gamma) - 18\beta(\lambda' T-1)(1+\gamma) + 36\beta(\lambda' T-1) \quad (2.6.6e)$$

$$m = \lambda\lambda'^3 T^3 \ell(1-4\gamma) - 3\lambda'^2 T^2(\lambda\lambda' T\ell+\beta) + 6\beta(\lambda' T-1)T\lambda'(1+2\gamma) + 6\beta(\lambda' T-1)(1+3\gamma) - 24\beta(\lambda' T-1) \quad (2.6.6f)$$

$$p = [-\lambda\lambda'^3 T^3 \ell + 3\lambda'^2 T^2(\lambda\lambda' T\ell+\beta) - 6\beta(\lambda' T-1)T\lambda' - 6\beta(\lambda' T-1)]\gamma + 6\beta(\lambda' T-1) \quad (2.6.6g)$$

$$q = \lambda\lambda'^4 T^4 \ell + 4\lambda'^3 T^3(\lambda\lambda' T\ell+\beta) + 12\beta T^3\lambda'^2(\lambda'-1/T) - 24\beta(\lambda'-1/T)T^2\lambda' - 24\beta(\lambda'-1/T)T(4+\gamma) + 120T(\lambda'-1/T) \quad (2.6.6h)$$

$$r = \lambda\lambda'^4 T^4 \ell(11-\gamma) + 4\lambda'^3 T^3(\lambda\lambda' T\ell+\beta)(3-\gamma) - 12\beta(\lambda'-1/T)T^3\lambda'^2(1+\gamma) + 24\beta(\lambda'-1/T)T^2\lambda'(3+\gamma) + 48\beta(\lambda'-1/T)T(3+2\gamma) - 240\beta(\lambda' T-1) \quad (2.6.6i)$$

$$u = 11\lambda\lambda'^4 T^4 \ell(1-\gamma) - 12\lambda'^3 T^3(\lambda\lambda' T\ell+\beta)(1+\gamma) + 12\beta(\lambda'-1/T) T^3\lambda'^2(\gamma-1) - 72\beta(\lambda'-1/T)T^2\lambda'(1+\gamma) - 48\beta(\lambda'-1/T)T(2+3\gamma) + 240\beta(\lambda' T-1) \quad (2.6.6j)$$

$$v = \lambda\lambda'^4 T^4 \ell(1-11\gamma) + 4\lambda'^3 T^3(\lambda\lambda' T\ell+\beta)(3\gamma-1) + 12\beta(\lambda' T-1)T^2\lambda'^2(1+\gamma) + 24\beta(\lambda' T-1)T\lambda'(1+3\gamma) + 24\beta(\lambda' T-1)(1+4\gamma) - 120\beta(\lambda' T-1) \quad (2.6.6k)$$

$$w = -[\lambda\lambda'^4T^4\ell+4\lambda'^3T^3(\lambda\lambda'T\ell+\beta)-12\beta(\lambda'T-1)T^2\lambda'^2$$
$$-24\beta(\lambda'T-1)T\lambda'-24\beta(\lambda'T-1)]\gamma+24\beta(\lambda'T-1) \qquad (2.6.61)$$

The overall system transfer function for the linearized hold is[2]:

$$\frac{N_z(z)}{N_o N_{dz}(z)} = \frac{3\lambda'TKz(2z-1)(az^2+bz+c)}{6\lambda'^4T\ell^2(z-1)^2(z-\gamma)+K(2z-1)(dz^3+ez^2+fz+g)} \qquad (2.6.7)$$

where all the constants are the same as defined for the system with the zero-order hold in equation (2.6.5).

Stability analysis of sampled data systems is performed by determining the zeros of the characteristic equation, that is, the denominator of equation (2.1.4), in the z plane. The criterion[6] is that the characteristic equation of the sampled data system have no zeros outside the unit circle, or, if λ_i denotes the ith root of the characteristic equation then:

$$|\lambda_i| \leq 1 \qquad (2.6.8)$$

Marciniak[2], using a program developed by Hafner[7], found the roots of the characteristic equations for all three types of hold for both a thermal and a fast reactor. Figures (2.6.1), (2.6.2) and (2.6.3) are the root locus plots of the characteristic equations of the system transfer functions of a theraml reactor for a zero-order, first-order and linearized hold respectively. (Based on results of Marciniak[2]). The sampling period is 0.1 second and the system parameters are as follows:

$$\lambda = 0.076 \text{ sec}^{-1}, \quad \beta = 0.0064, \quad \ell = 10^{-3} \text{ sec} \qquad (2.6.9)$$

Examination of equations (2.6.5), (2.6.6) and (2.6.7) shows that T and K are the only variables for a fixed reactor. T is the

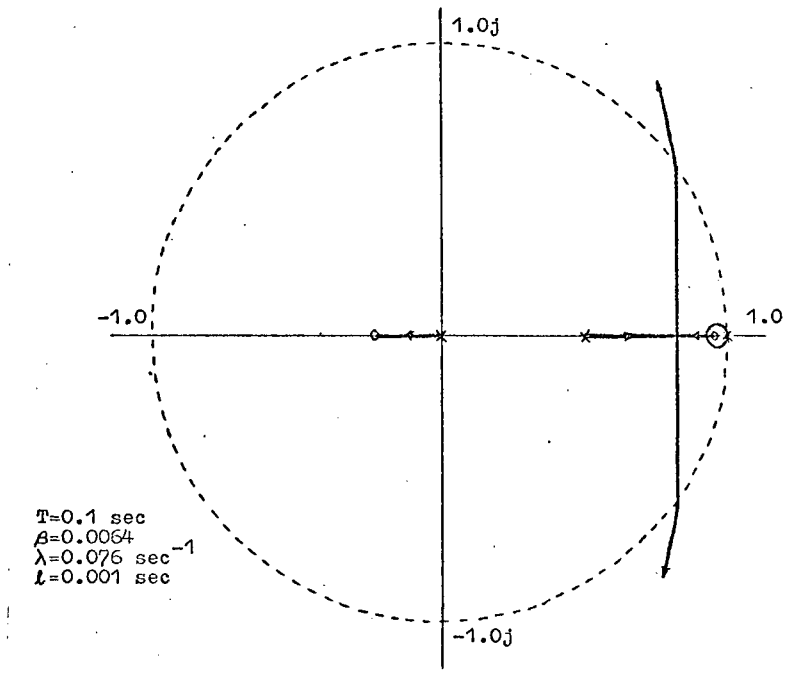

Fig. 2.6.1 Root Locus Plot of a Thermal Reactor Sampled Data Control System with Zero-Order Hold

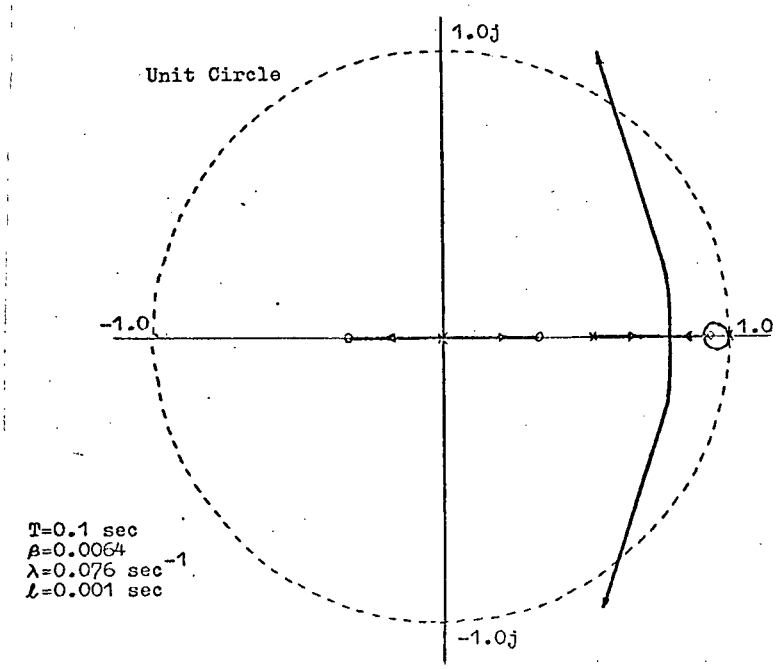

Fig. 2.6.2 Root Locus Plot of a Thermal Reactor Sampled Data Control System with First-Order Hold

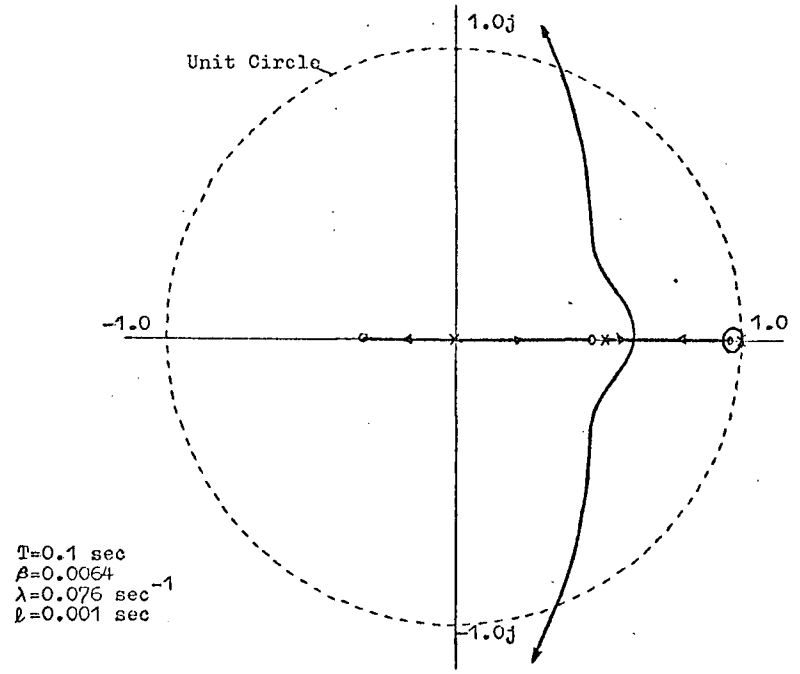

Fig. 2.6.3 Root Locus Plot of a Thermal Reactor Sampled Data Control System with Linearized Hold

sample period and K is the reactivity rate per unit error per neutron lifetime, i.e.

$$K = R/\ell \tag{2.6.10}$$

But ℓ is fixed for a certain reactor, therefore a sampled data reactor system of the form of figure (2.1.4) can be said to be stable for a specific sample period T, provided the reactivity rate per unit error R is less than a critical value R_{max}. The value R_{max} ensures that all poles of the characteristic equation lie within the unit circle in the z plane. The unit error E_u is defined as:

$$E_u = E/N_o \tag{2.6.11}$$

Marciniak[2] has drawn up tables of R_{max} versus sample period T for various reactor types. Table (2.6.1) gives the maximum allowable reactivity rate per unit error for various sample periods for the reactor with parameters as in equation (2.6.9). From this table it can be seen that the zero-order hold is the most stable except for the 0.1 second sampling period.

Sample Period	Reactivity Rate (% δ k/k) / sec		
T (sec.)	Zero-Order Hold	First-Order Hold	Linearized Hold
0.1	7.4	8.3	8.4
0.5	1.83	1.45	1.2
1.0	0.99	0.73	0.62
5.0	0.173	0.14	0.123

Table 2.6.1 Maximum Allowable Reactivity Rate R_{max} per Unit Error to Ensure Stability versus Sampled Period. (Thermal Reactor)

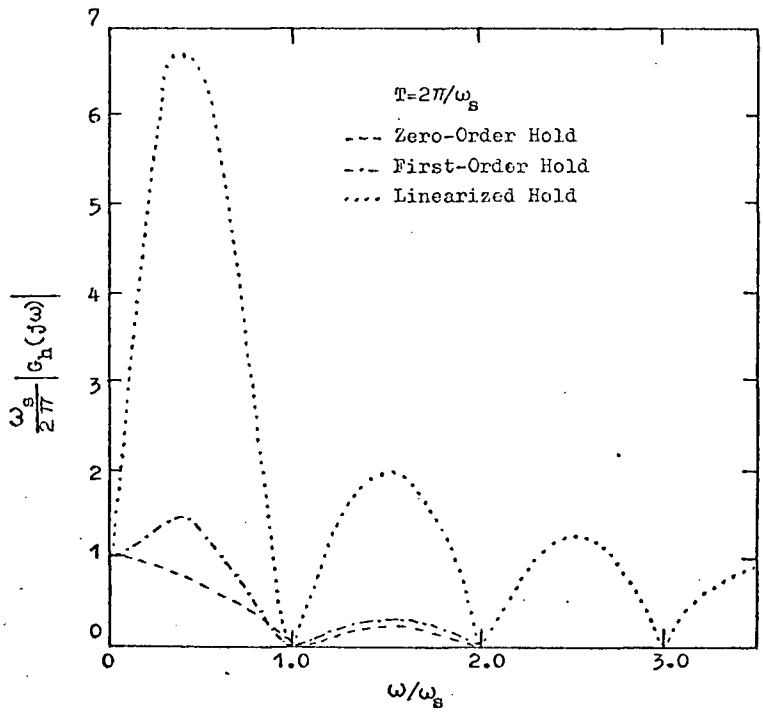

Fig. 2.6.4 Amplitude versus Frequency for Zero-Order, First-Order, and Linearized Holds.

Figure (2.6.4) shows the amplitude versus frequency curves for the three holds. Compared to the zero-order and first-order holds, the linearized hold does not act as a very good filter in that it amplifies frequencies greater than the sampling frequency. There is also considerable amplification of frequencies less than the sampling frequency with a fairly steep cut off. Examination of figure (2.6.5),

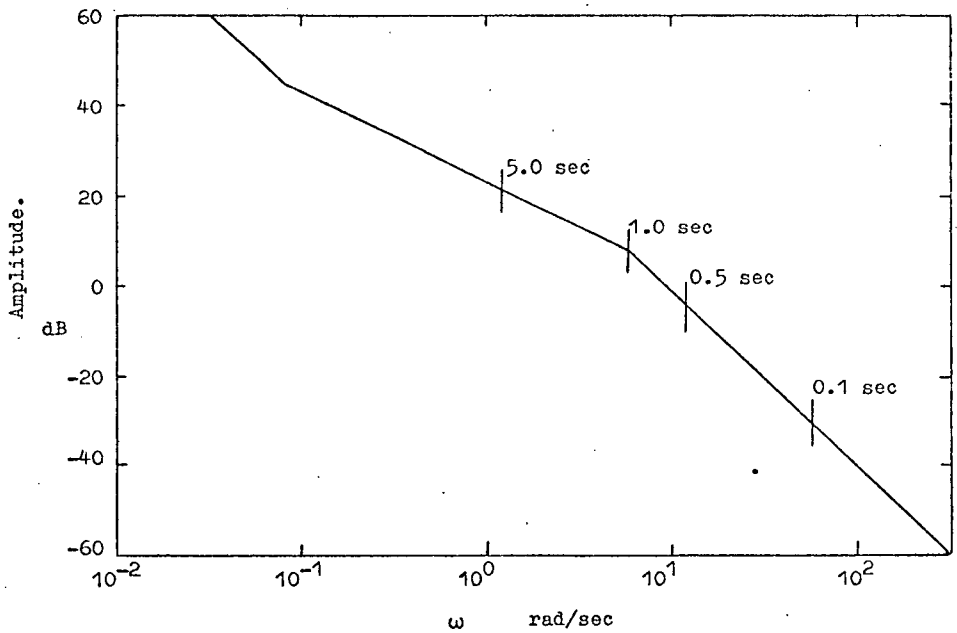

Fig. 2.6.5 Bode Plot of Thermal Reactor plus Control Rod Servo System.

the Bode plot of the reactor plus control rod, shows that with a 0.1 second sample period the high frequency components are not readily passed by any type of hold, as these components have an amplitude of the order of -35 dB. However, with longer sample periods, frequencies above the sample frequency are amplified by the linearized hold, making the system less stable. Therefore the linearized hold should be used only for sample periods in the order of 0.1 second and the zero-order should be used for all longer sample periods.

In Chapter 3 it will be shown that the results of the stability analysis using linear power levels are applicable to the logarithmic power level control algorithm developed in that Chapter. In Chapter 5 the controller is tested using analog and digital simulations and it will be seen that the results of Table 2.6.1 have a 25% safety margin.

3. DIRECT DIGITAL CONTROL ALGORITHM

The digital control algorithm besides maintaining the reactor at a steady state must also be able to change the neutron power from one demand level to another as quickly and as safely as possible with a minimum of over- or undershoot of the final demand level. For safety reasons the rate at which the neutron power level can change is constrained and any such power level change must be carefully controlled. In this chapter a summary of previous algorithms will be given, followed by the development of an algorithm based on logarithmic power level that results in much quicker and simpler computer calculations. All algorithms are based on the error sampled closed loop control system described in Chapter 2. Time optimal digital control will be covered in Chapter 4, although allowances for its inclusion will be made in this chapter.

3.1 Constraints on Demand Power Level Changes

As mentioned in section 2.1, the input to the reactor control system of figure (2.1.4) is a demand power level plus a constraint on the minimum allowable reactor period for safety reasons. This minimum period constraint is only applicable to increases in power level. The demand power level N_d must therefore be constrained such that:

$$N_d[(n+1)T] \leq N_d(nT) \quad \exp\ (T/\tau) \qquad (3.1.1)$$

where

T = sample period

and τ = minimum allowable period

However, during power level decreases, it is often desirable to constrain the negative reactor period to prevent the control rods from being inserted too far, which would result in tremendous undershoot of the final

demand level such that

$$N_d[(n+1)T] \geq N_d(nT) \exp(T/-\tau_s) \qquad (3.1.2)$$

where τ_s is the demanded period for power decreases.

Reactors of any appreciable power often have a constraint imposed upon them by the thermal system in the form of a linear rate constraint so that[8]:

$$N_d(nT) - \Delta N \leq N_d[(n+1)T] \leq N_d(nT) + \Delta N \qquad (3.1.3)$$

where

$$\Delta N = \left|\frac{dN}{dt}\right|_{max} \qquad (3.1.4)$$

The digital control algorithm, besides maintaining the reactor level must thus also be able to increase or decrease the reactor power level within the above constraints. In Chapter 4, time optimal control is handled and this too will impose some constraints on the reactor period.

3.2 Summary of Existing Algorithms

Cohn[3] proposed a digital control algorithm in 1966 which was later modified by Marciniak[2]. The hold used was the linearized hold analysed in section 2.2.1 where

$$E'(t) = N'_d - N_f = N'_d - N_p^2/N_1, \quad nT \leq t \leq (n+1)T \qquad (3.2.1)$$

and

$E'(t)$ = error

$N'_d = N_d[(n+1)T]$

= demand flux level of next sampling

$N_1 = N[(n-1)T]$

= measured flux level of last sampling

$N_p = N(nT)$

= measured flux level of present sampling

$N_f = N'[(n+1)T]$

= expected flux level of next sampling if no control action taken from present to next sampling.

The algorithms were only developed for power increases and the flux demand was given by:

$$N'_d = \min [N_p + K, N_d \exp(T/\tau), N_e] \qquad (3.2.2)$$

where K = constant

T = sample period

τ = demanded reactor period

N_e = final flux endpoint

The first argument (N_p+K) ensures that in the initial stages the demand does not diverge too far from the actual flux preventing excessively rapid rises at a later stage. Only bang-bang control action was used and if the error exceeded a certain deadband, the control rods were driven full speed in or out depending on the error sign.

Nuclear reactors have a range covering many decades and this has resulted in the use of floating point arithmetic for the control algorithm calculations. Cohn[9] tested the speeds of a selection of small computers and discovered that for computers with hardware fixed point arithmetic units the time for an addition is in the order of 0.5 to 1.0 msec. Multiplication and division times are also from 0.5 to 1.0 msec, with the logarithmic and sine function times in the order of 5.0 to 10 msec. The computer is not only responsible for the control of the reactor power level but also for other functions such as safety interlocks and safety scanning, data logging and the control of other system components. This has meant that the maximum sample rate has often been set by the time taken in the calculation of the control algorithm and other duties instead

of a desired faster sample frequency. In section 2.6 it was shown that the sample period set a maximum rate of reactivity change per unit error to ensure stability and thus the higher the sample rate the greater the stability margin. There is still some controversy over high sample rates due to the greater frequency of movement of the control rods. However, a sample rate of 10Hz has now been accepted as the maximum acceptable sample rate. Besides the use of floating point arithmetic resulting in a reduction in the sampling frequency, there is also the delay between the measurement of the reactor power and the actual output of control action which makes the system less stable. This delay has not been taken into account in the section on stability analysis (section 2.6). In the extreme, the sampling of the neutron power level can immediately follow the output of control action from the last sampling. In the next sub-section, it will be shown how the use of logarithmic power levels can allow the use of fixed point arithmetic, greatly increasing the algorithm calculation speed.

Examination of equation (2.4.1) shows that the gain of a reactor is proportional to the neutron power level such that

$$A = K'N_o \qquad (3.2.3)$$

where A = total gain

K' = gain constant

N_o = actual power level

In order to hold the overall system gain constant, a gain term of the order $1/N_o$ must be added to the error sampler. Cohn[3] in his system did this by varying the error deadband in proportion to the neutron power level. Using logarithmic power levels will be seen to compensate the gain automatically.

3.3 Logarithmic Digital Control Algorithm

Taking the case of the zero order hold define

$$\varepsilon(t) = \ln E_1(t) = \ln N_d(nT) - \ln N(nT)$$
$$nT < t \leq (n+1)T \qquad (3.3.1)$$

instead of the normal linear case of

$$E(t) = N_d(nT) - N(nT), \qquad nT < t \leq (n+1)T \qquad (3.3.2)$$

as given in equation (2.2.3). Therefore

$$E_1(t) = N_d(nT)/N(nT), \qquad nT < t \leq (n+1)T \qquad (3.3.3)$$

Let

$$E_1(t) = 1 + \Delta \qquad (3.3.4)$$

Using the approximation that

$$\ln (1 + \Delta) \approx \Delta \quad \text{for } |\Delta| << |1| \qquad (3.3.5)$$

then $$\varepsilon(t) \approx \Delta \qquad (3.3.6)$$

as N(nT) must deviate only slightly from $N_d(nT)$. Substitution in equation (3.3.4) gives

$$E_1(t) = 1 + \varepsilon(t), \quad nT < t \leq (n+1)T \qquad (3.3.7)$$

Dividing equation (3.2.3) by N(nT) gives

$$\frac{E(t)}{N(nT)} = \frac{N_d(nT)}{N(nT)} - 1 \qquad (3.3.8)$$

From equations (3.3.3) and (3.3.7)

$$\frac{E(t)}{N(nT)} = E_1(t) - 1 \qquad (3.3.9)$$

$$= \varepsilon(t), \qquad nT < t \leq (n+1)T \qquad (3.3.10)$$

For the first order hold the logarithmic error is defined as follows:

$$\varepsilon(t) = \varepsilon(nT) + (\varepsilon(nT) - \varepsilon((n-1)T))\ (t-nT)/T,$$
$$nT < t \leq (n+1)T \qquad (3.3.11)$$

where $\varepsilon(nT) = \ln N_d(nT) - \ln N(nT)$

The error of the linearized hold using logarithmic power levels is defined as follows:

$$\varepsilon(t) = \ln N_d[(n+1)T] - 2 \ln N(nT) + \ln N[(n-1)T],$$

$$nT < t \leq (n+1)T \qquad (3.3.12)$$

Again it is easy to prove that for the first-order and linearized holds that

$$\varepsilon(t) = E(t)/N(nT), \qquad nT < t \leq (n+1)T \qquad (3.3.13)$$

where $\varepsilon(t)$ is the error using logarithmic power levels and $E(t)$ is the error using linear power levels.

The unit error that was defined in section 2.6 is the same as equation (3.3.13), therefore the stability analysis of that section applies to the logarithmic control algorithm as well. Cohn[3] in his system compensated for the non linear gain of the reactor by varying the deadband in proportion to the neutron power. From equation (3.3.13) it can be seen that the logarithmic error sampler automatically compensates for this gain variation.

The range of power of a reactor can vary from a minimum of 6 decades for heavy water moderated reactors to as much as 14 decades for graphite reactors. It is this extreme range that has made floating point arithmetic necessary. When using logarithmic power levels this range is reduced to 14 for the case of the graphite reactor making it possible to use fixed point arithmetic with tremendous increases in calculation speeds. In Chapter 5, a PDP-9 computer was used to test experimentally the control algorithm. The total time elapse from the reading of the neutron power level to the output of the control action was twice the time taken for one addition using the floating point package

of the computer.

3.4 Logarithmic Digital Control Algorithm Demand Power Level Changes

In section 3.1 the constraints on the change in reactor power level were seen to be a minimum allowable reactor period constraint and a linear rate constraint. Time optimal control (which is covered in the next chapter) imposes a constraint on the minimal allowable reactor period as the final endpoint is approached, so that there is minimal over- or undershoot. The demand power level at the next sampling is given as:

$$N_d[(n+1)T] = N_d(nT) \exp (T/\tau_d) \tag{3.4.1}$$

Therefore

$$\ln N_d [(n+1)T] = \ln N_d (nT) + T/\tau_d \tag{3.4.2}$$

where τ_d = demanded reactor period.

Let

τ_m = minimum allowable reactor period

τ_1 = minimum allowable reactor period as imposed by the linear rate constraint

$$= N(nT)/\Delta N \tag{3.4.3}$$

where $$\Delta N = \left| \frac{dN}{dt} \right| \quad \max \tag{3.4.4}$$

and τ_o = minimum allowable reactor period as imposed by the time optimal constraint.

Then $$\tau_d = \max [\tau_m, \tau_1, \tau_o] \tag{3.4.5}$$

For the case when $\ln N_d (nT) < \ln N_e$, that is a power level increase, where N_e is the final endpoint, then

$$\ln N_d[(n+1)T] = \min [\ln N(nT) + C, \ln N_d(nT) + T/\tau_d, \ln N_e] \tag{3.4.6}$$

where C = constant. (3.4.7)

Constant C is chosen somewhere in the order of twice the error which gives full control rod velocity.

The power demand ($\ln N_d$) is used for the calculation of the next power demand point instead of ($\ln N$), to ensure that the demand will rise smoothly, unaffected by the statistical fluctuations in ($\ln N$). However, the first term ensures that the demand will not diverge too far from the actual power in the initial stages of the power level increase, when the power is rising much more slowly than the demand, thus preventing excessively rapid rises at a later stage.

If there is a decrease in power level, that is $\ln N_d(nT) > \ln N_e$, then

$$\ln N_d[(n+1)T] = \max [\ln N(nT) - C, \ln N_d(nT) - T/\tau_d, \ln N_e] \quad (3.4.8)$$

Equations (3.4.6) and (3.4.8) will be used in the development of a practical digital controller in Chapter 4.

3.5 Logarithmic Power Level Measuring Circuits

Two possible methods of measuring the logarithmic power level are as follows:

a) The same circuits as in section 2.5 can be used and the logarithm of the power calculated digitally;

b) The ion chamber amplifiers of figures (2.5.1) and (2.5.2) can be replaced by logarithmic ion chamber amplifiers. Exceptionally good logarithmic amplifiers covering up to seven decades are now available. This method is preferable to (a) as it provides a much more even spread of digitized logarithmic power levels besides requiring fewer measuring ranges to cover the entire power operating range.

4. TIME OPTIMAL REACTOR CONTROL

Due to the approximate nature of the models used in time optimal control studies, practical applications to real or simulated systems normally result in sub-optimal control. This is especially true of reactor systems which are highly non-linear and complex. Safety standards impose many constraints upon reactor operation, making optimal control more complicated. Studies in time optimal digital control of nuclear reactors have thus resulted in time consuming computer calculations of high complexity. In this section, optimal control sequences using switch points will be developed. Simulation techniques will be used in obtaining the switch points, thereby eliminating the complex and very approximate calculations.

4.1 Review of Present Literature

Much has been published in the past twenty years concerning the optimization of continuous and sampled-data control systems. Most notable of these endeavours are the more general theories advanced by Pontryagin et al.[10] and Bellman[11]. Only in recent years has much attention been focused on the optimization of nuclear systems, especially in the optimal shutdown of reactors to avoid the poisoning of the reactor by Xenon build up. Literature on the design of optimal digital or sampled-data control systems for nuclear reactors is sparse.

A series of papers published by Monta[12,13,14] was one of the first complete studies on the optimization of continuous as well as discrete reactor systems. The analysis was based on the calculation of the reactivity using a prompt-jump approximation[12]. This approximation was proven to be inadequate as the reactor, when set for a 25 sec. minimum period, increased with an unsafe 16 sec. period. A side effect was

that the minimum sample frequency possible was 0.5 Hz, due to the calculation time. Lipinski[4], who has made a complete literature study of papers pertaining to nuclear reactor control systems, proposed a linear deterministic system using a Kalman filter. The results from this system were extremely good; however they were idealistic, because the reactivity and delayed neutron precursor densities were required at each sampling instant, resulting in long calculation times. It was suggested that a hybrid computer system be used, with the analog portion solving the differential equations in order to speed up the calculation time. These studies did not include all the constraints imposed on a nuclear reactor such as minimum allowable period, the maximum rate of reactivity insertion and linear rate constraints. With their inclusion, the complexity of the optimum control algorithms can only be expected to increase. Since total optimization of the control of a nuclear plant includes the overall performance and cost of the controller as well, the question is raised whether sub-optimum performance of the reactor is not desirable. With so little practical experience at present with actual sampled data reactor control systems, this question is difficult to answer and might form the basis of an interesting future investigation. Marciniak[2] studied the problem from the side of the constraints imposed upon the system by safety regulations. This study seems to be most applicable to practical applications and will form the basis of a time optimal study using the logarithmic digital control algorithm developed in the previous chapter.

4.2 Time Optimal Power Increases

For power increases it is desirable that the minimum allowable reactor period constraint be adhered to and that there be a minimum of

overshoot. There is also the constraint on the maximum allowable reactivity rate imposed either by stability or mechanical design requirements. Taking these into account Marciniak[2] applied the Maximum Principle of Pontryagin[10] to obtain an optimal control sequence for reactor power increases. For the case where the delayed neutron precursors are ignored, the sequence is as in figure (4.2.1). The control rods are withdrawn at full speed until the demanded minimum period is obtained and the reactivity is then held constant. At a switch point S_m the control rods are inserted at full speed such that as the final demand level is reached, the total

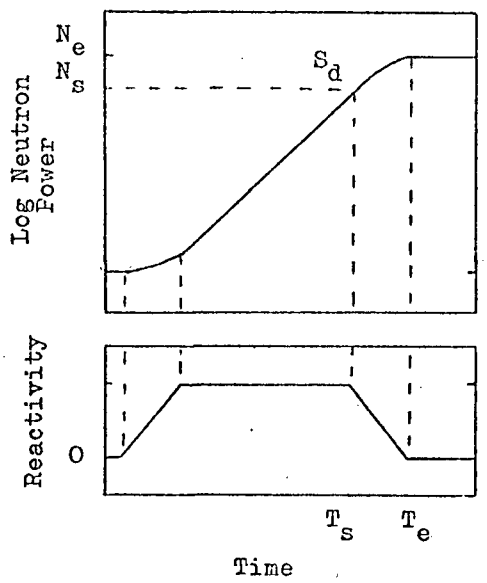

Fig. 4.2.1 Time Optimal Control Sequence for Prompt Reactor.

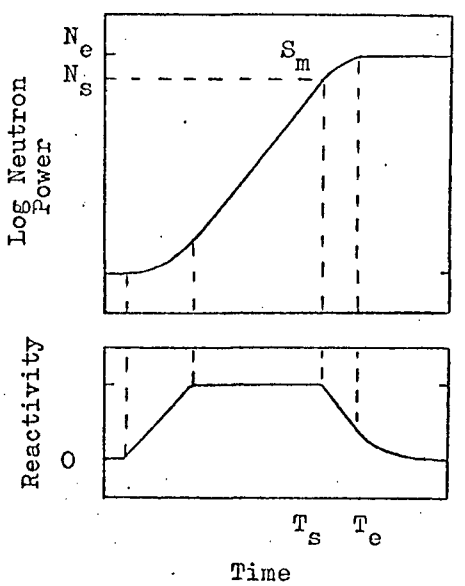

Fig. 4.2.2 Time Optimal Control Sequence with Delayed Neutrons Included.

reactivity is zero. Taking one group of delayed neutrons into account resulted in the sequence as given in figure (4.2.2). Again the control rods are withdrawn from the reactor at full velocity until the demand period is obtained after which the reactivity is held constant. At a switch point S_d, the control rods are inserted at maximum rate until the final demand is reached. However, on reaching the final demand, the total reactivity is not zero, and the reactivity is now decreased exponentially,

maintaining the endpoint level. When the endpoint is reached, the delayed neutrons are not in equilibrium for the endpoint level and the power level is held constant by the variation of the reactivity while precursor-density equilibrium is attained. The variation of the reactivity to maintain the final demand level can be obtained as follows:

The one delayed group kinetics equations as given in Appendix A are

$$\frac{dn}{dt} = \frac{u - \beta}{\ell} n + \lambda C \tag{4.2.1}$$

and

$$\frac{dC}{dt} = \frac{\beta}{\ell} n - \lambda C \tag{4.2.2}$$

where u = the reactivity or control.

Solving for u(t), when dn/dt is zero gives

$$u(t) = \beta - (\lambda \ell C(t)/n_e) \tag{4.2.3}$$

where n_e is the final demand level.

Harrer[15] showed that the ratio of C to n when the reactor is on an asymptotic period T can be given by

$$\frac{C}{n} = \frac{\beta}{\ell(\lambda + 1/\tau)} \tag{4.2.4}$$

Therefore if it is assumed that the reactor is on an asymptotic period τ_e when the final demand level n_e is reached, then:

$$C_e = \frac{n_e \beta}{\ell(\lambda + 1/\tau_e)} \tag{4.2.5}$$

Solving the differential equation (4.2.2) for when the demand level n_e is reached, gives

$$C(t) = \frac{\beta n_e}{\lambda \ell} \left\{ 1 - \frac{\exp[-\lambda(t-t_e)]}{(\lambda \tau_e + 1)} \right\} \tag{4.2.6}$$

where t_e is the time when the demand level n_e was reached. Substituting

for C(t) into equation (4.2.3) gives

$$u(t) = \frac{\beta}{(\lambda\tau_e + 1)} \exp\ [-\lambda(t-t_e)] \qquad (4.2.7)$$

Differentiation gives the reactivity rate

$$\frac{du(t)}{dt} = \frac{-\beta\lambda}{(\lambda\tau_e + 1)} \exp\ [-\lambda(t-t_e)] \qquad (4.2.8)$$

The maximum reactivity rate is needed precisely at the time the final demand level is reached, thus if the maximum reactivity rate is known, the minimum allowable asymptotic period τ_e at the instant the final demand level n_e is reached, can be calculated to ensure no overshoot.

Therefore, from (4.2.8) $$R_{max} = \frac{\lambda\beta}{\lambda\tau_e + 1} \qquad (4.2.9)$$

and $$\tau_e = \frac{\beta}{R_{max}} - \frac{1}{\lambda} \qquad (4.2.10)$$

where R_{max} is the maximum rate of reactivity.

As the maximum reactivity rate is normally known for a particular reactor, as well as the minimum allowable period, a check using equation (4.2.9) or (4.2.10) can verify whether the calculation of a switch point S_d is necessary.

Examination of equation (4.2.3) shows that the final demand power level can only be held constant when

$$R_{max} \geq \left|\frac{\lambda\ell}{n_e} \frac{dC}{dt}\right| \qquad (4.2.11)$$

Due to the non-linear nature of reactors, the easiest method for determining the switch point S_d is by simulation methods. In Chapter 5, a digital simulation of a zero-order, six delayed group, point kinetics model is used for testing of the digital controller. The simulated

reactor is set on a power increase and brought to the desired demand period with the aid of the controller.

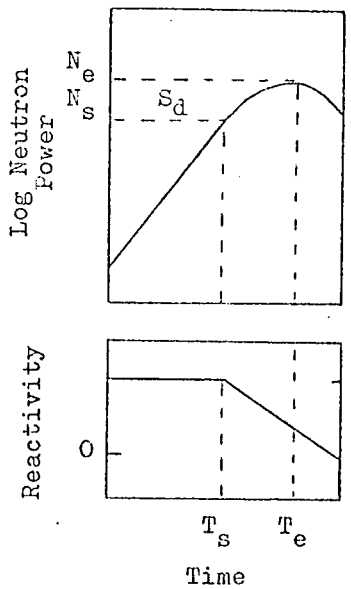

Fig. 4.2.3 Time Optimal Control Switch Point Calculation

When an asymptotic period has been attained, the control rods are inserted at full speed. The condition of equation (4.2.11) is met when the peak power value N_e is reached, as in figure (4.2.3). The switch point can be determined in the form of a ratio of N_s to N_e where N_s is the power level at the switch point. Table (4.2.1) gives the ratio of N_s to N_e for various minimum allowable periods and maximum reactivity rates for the thermal reactor simulated in Chapter 5.

Reactor Period (sec).	SWITCH POINT N_s/N_e				
	0.2mk/sec. max rate	0.1mk/sec. max rate	0.05mk/sec. max rate	0.02mk/sec. max rate	0.01mk/sec. max rate
20	0.983	0.922	0.726	0.278	0.048
30	-	0.976	0.885	0.549	0.213
40	-	-	0.943	0.722	0.400
50	-	-	0.971	0.814	0.548
100	-	-	-	0.966	0.880

Table 4.2.1 Time Optimal Switch Points For Power Increases

Marciniak[2] developed the switch equation

$$\frac{N_s}{N_e} = \left\{ b + cd + b(1-d)\frac{C_o}{N_o} + \left[\frac{c}{\ell a}(1-d) + \frac{b}{\ell} t_\Delta\right] u_s + R_{max}\left[\frac{c}{\ell a}\left(t - \frac{1-d}{a}\right) + \frac{b}{2\ell} t_\Delta^2\right]\right\}^{-1} \qquad (4.2.12)$$

where

$a = \lambda + \beta/\ell$

$b = \lambda/a$

$c = \beta/\ell a$

$d = \exp(-at_\Delta)$

u_o = total reactivity at the switch point S_d

t_Δ = time interval from the switch point to the final demand level

and where t_Δ is calculated by assuming that when the final demand is reached, the period is asymptotic. Making use of the relationship between asymptotic period and reactivity developed by Glasstone[16] where the reactivity u in terms of the period τ is

$$u = \frac{\beta}{(\lambda\tau + 1)} \tag{4.2.13}$$

as well as

$$u_e = u_s - R_{max}(t_\Delta) \tag{4.2.14}$$

the time interval is

$$t_\Delta = \frac{\beta}{R_{max}}\left[\frac{1}{(\lambda\tau_s + 1)} - \frac{1}{(\lambda\tau_e + 1)}\right] \tag{4.2.15}$$

In the derivation of equation (4.2.12), use was made of the linearized one delayed group kinetics equation (See Appendix A), where

$$\frac{dn}{dt} = -\frac{\beta n}{\ell} + \lambda C + \frac{un_o}{\ell} \tag{4.2.16}$$

This equation is only valid in the vicinity of n_o. As a result, equation (4.2.12) is only reliable for switch points in the vicinity of the final demand level which is the case for minimum periods greater than 80 to 100 seconds or for reactors with large maximum reactivity rates.

In Chapter 5, a practical digital controller is developed and

use will be made of the switch point for time optimal control.

4.3 Time Optimal Power Decreases

The optimal shut-down of reactors has been well covered in optimal reactor control studies[17,18,19,20] and will not be covered here. Therefore, for reactor shut-downs, where the control of the xenon poisoning is required, the demand power level of the reactor will be programmed according to a time optimal sequence as given in the above references. The occasion could arise, however, when it is required to reduce the reactor power to a predetermined level for a short period of time, such that the xenon poisoning problem can be disregarded. Glasstone[16] has shown that it is not possible to reduce the neutron flux in a reactor more rapidly than is permitted by the most delayed neutron group with the relationship between the reactivity u and period τ given as follows:

$$u = \frac{\beta}{1 + \lambda_1 \tau} \qquad (4.3.1)$$

where λ_1 is the decay constant of the group having the precursor of longest life. As u increases numerically, $(1 + \lambda_1 \tau) \to 0$, thus for large negative reactivities the stable period τ approaches $1/\lambda_1$. It must be noted that β is larger than usual since the delayed neutrons now constitute a greater proportion of the fission neutrons. For most reactors, λ_1 is in the order of 0.0125 sec^{-1}, therefore the stable period for large negative reactivities tends towards 80 seconds. Due to the constraint on the reactivity rate, it has thus been customary to constrain the maximum amount of negative reactivity in order to prevent tremendous undershoots of the final demand level. A second method is to limit the allowable negative reactor period for power decreases. Figure (4.3.1) shows a simple sub-optimal power decrease control sequence with a con-

straint on the minimum allowable negative period. The effect of the precursor with longest delay time can be clearly seen, as more than 10 minutes is required for a stable asymptotic period of 100 seconds to be attained. At a switch point S_s the reactivity is inserted at maximum

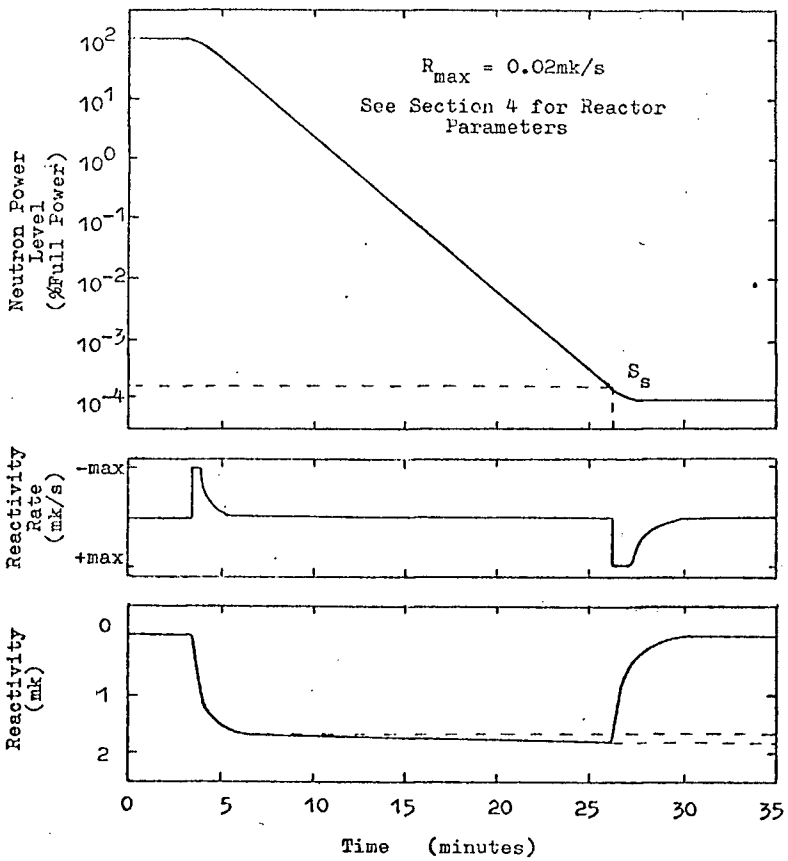

Fig. 4.3.1 Power Decrease with 100 Second Period Constraint

rate until the final demand level is reached. As was seen in the case for power increases, when the endpoint is reached, the reactivity is not zero. The power level is held constant by the variation of the reactivity while precursor-density equilibrium is attained. Calculation of the switch point S_s is complex, with many approximations and assumptions. Again the easiest method is by simulation techniques. A minimum negative reactor period of the order of 100 seconds is suitable, as it requires only 1.6 to 2.0 mk to maintain it on a stable period (see figure 4.3.1)

and does not differ too much from the 80 second limit. The main problem is that the power level has decreased by as much as six decades before a stable asymptotic period is attained. However, if the switch point is determined when this period has been attained, it will be conservative for power decreases of fewer decades as far as undershoot is concerned. Using the digital simulation and controller of Chapter 5, with a 100 second minimum allowable reactor period for power decreases, and a maximum reactivity rate of 0.02mk/s, the ratio of switch point level N_s to the final endpoint N_e is 1.188.

In the next chapter, the switch points will be used in the development of a practical digital controller which permits fairly good approximations to the time optimal control sequences outlined in the previous sub-sections.

5. PRACTICAL DEMAND POWER LEVEL CONTROLLER

A practical digital controller is developed using machine language programming and incorporating the time optimal sequence switch points outlined in Chapter 4. Digital and analog simulations of a thermal reactor are used to test the controller for overall stability as well as for controlled power level changes with various minimum allowable periods and reactivity rates.

5.1 Control Computer Specifications and Programming

As mentioned in Chapter 1, the basic power level controller will be assumed to be part of a much larger system consisting of a number of mass storage units and mini-computers assigned their own particular tasks.

The control computer must therefore be able to communicate with the other system computers as well as read from and write to the mass storage units. A hardware fixed point arithmetic unit option must be installed in the computer. If output of control action is directly from the basic controller then the necessary equipment must be interfaced to the computer.

The range of a nuclear reactor can extend over more than fourteen decades, although under normal operating conditions this would be in the order of six to ten decades, depending on the reactor type. However, it is convenient to have the computer extending over the widest range possible, especially for initial startups and long term shutdowns. Calculation speed is important, and as floating point arithmetic units for mini-computers are not readily available, the logarithmic control alogarithm was developed in Chapter 3, making the use of fixed point

arithmetic possible. Of the variables for the algorithm, the demand power level requires the greatest precision. From equation (3.4.2) the logarithmic power level is

$$\ln N_d\left[(n+1)T\right] = \ln N_d(nT) + T/\tau_d \qquad (5.1.1)$$

or for the $\log_{10}$ case

$$\log N_d\left[(n+1)T\right] = \log N_d(nT) + (T/\tau_d)\ \log\ (e) \qquad (5.1.2)$$

The minimum likely sample period T is 0.1 second (see section 3.2). If the smallest maximum rate of reactivity change R_{max} is 0.01 mk/sec., then from equation (4.2.10) the longest probable period for power changes is 630 secs. This period gives a minimum linear rate constraint of 0.16% full power per second which is more than adequate. Therefore

$$\left[(T/\tau_d)\ \log(e)\right]\ \min = (0.1/160)\ 0.435 \qquad (5.1.3)$$

$$= 6.8 \times 10^{-5} \qquad (5.1.4)$$

Assuming a 1% accuracy for these extremely long periods and taking the 16 decade power range into account gives a precision requirement for $\log N_d$ of nine decimal digits or thirty bits. This is an extreme maximum limit. On the other hand it might only be possible to obtain a spread of 1000 sample points per decade. Assuming a calculation accuracy of 1%, this gives a precision requirement of seven decimal digits or twenty-three bits. The word length of most mini-computers is 12, 16, 18 and 24 bits. Therefore, for most machines, double precision fixed point arithmetic is necessary. Depending on the sample period, the power range, accuracy of calculations and maximum required reactor period, it might be possible to use single precision arithmetic with the 24 bit machines, which has many advantages. In the development of a practical digital

controller, a Digital Equipment Corporation PDP-9[21] computer with a word length of 18 bits was used. This computer is linked to an EAI 231R[22] analog computer to form a hybrid facility. The hybrid interface was originally developed by Marston[23] with a software package being developed by Crawley[24].

Most mini-computers are supplied with comprehensive soft-ware packages, including a basic operating system, Fortran, an assembler, editor and loaders. The development of an overall operating system will not be dealt with in this thesis. In previous reactor control system programming, much use has been made of Fortran, due partly to the requirement of floating point arithmetic. Use of machine language programming usually results in much faster and smaller programs in core space than would be attained with Fortran programming. Throughout the development of a practical digital controller the PDP-9 Assembly language was used. After examination of the precision and mathematical functions required, a double precision fixed point two's complement arithmetic package was developed. The sub-routines in the package and their calculation speeds are given in table 5.1.1. Comparison of the calculation speeds with those found by Cohn[9] show how much faster the fixed point routines are than their floating point equivalents. Part of the software support package for the PDP-9 is a macro-assembler[25] which can simplify tedious machine language programming. A macro definition file was developed for the calling of the above sub-routines and includes conditional as well as single precision arithmetic macros. The form of the macros is as follows:

LABEL FUNCTION VARIABLE 1, VARIABLE 2, (ANSWER OR CONDITIONAL JUMP ADDRESS)

Using these macros makes programming much simpler and more reliable as well as eliminating many pitfalls for the inexperienced machine language programmer.

Function	Calculation Time (μsec)	
	Fixed Point	Floating Point*
Two's Complement	37	-
Addition	48	500
Subtraction	55	550
Positive Multiply	130	500
Signed Multiply	245	500
Fractional Positive Multiply	70	-
Fractional Signed Multiply	190	-
Logarithm**	183	4770
Antilog**	230	-
Ten Power X**	140	-

* See Reference 9

** See Reference 26 for Algorithms

Table 5.1.1 Arithmetic Sub-routine Functions and Calculation Times

5.2 Demand Power Level Controller

A flow diagram of the basic power level controller is shown in figure (5.2.1). On the sample period interrupt, the neutron power is sampled and if more than one circuit is used, the readings are then averaged. If the readings are in linear form, the logarithmic value is found and then scaled and calibrated. The error between the demanded flux at that sampling and the actual flux is determined and the

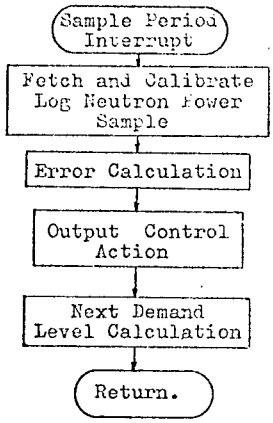

Fig. 5.2.1 Basic Controller Flow Diagram

necessary action is output to the control rods. The demanded flux for the next sampling is then calculated before exiting from the routine. By far the longest calculation is for the demand power at the next sampling and it is calculated last, so that the output of control action occurs as soon as possible after sampling the neutron power. In the following sub-sections, each phase of the algorithm will be dealt with in detail.

5.2.1 Fetching of Neutron Power Sample

The precise manner is which the neutron power is sampled will depend on the overall system configuration. If a separate computer is used for data acquisition and logging, as in Chapter 1, it can transfer the averaged power level to the demand power level controller and then interrupt it. If logarithmic conversion, scaling and calibration are required this can take place in either computer. If possible, logarithmic ion chamber amplifiers should be used so that the logarithmic neutron level can be sampled directly, as well as providing an even spread of digitized power levels (see figures (2.5.1) and (2.5.2)). Excellent logarithmic amplifiers covering up to seven decades are now available[27]. No matter which type of amplifier is used, it will be necessary to divide the entire power level span into overlapping measuring ranges as in figure (5.2.2). The transition from one range to the next is given by

$$N = (1-\alpha)\, N_l + \alpha N_u \qquad (5.2.1)$$

where N is the power level, N_l is the reading from the lower range, N_u is the reading from the upper range and α is as in figure (5.2.2).

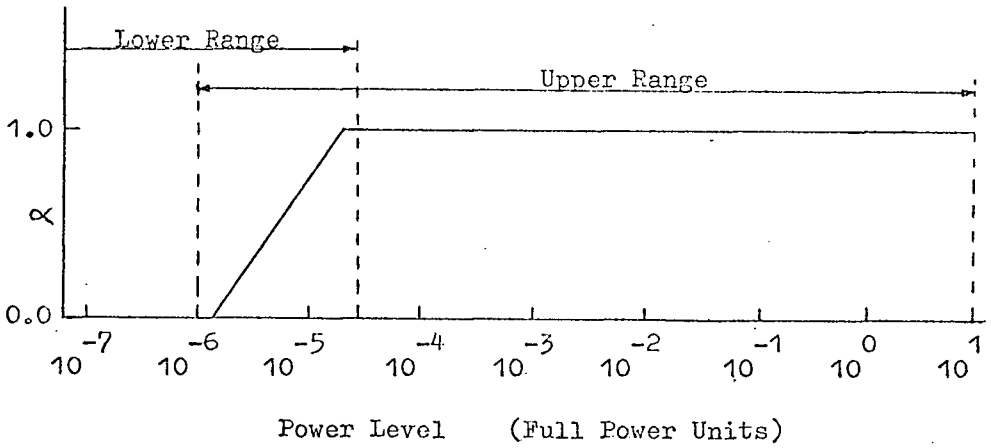

Fig. 5.2.2 Merging of Upper and Lower Measuring Ranges

In the test of the controller using the digital simulation, this stage is omitted as the simulation transfers the logarithmic neutron power level directly to the controller. Using the analog simulation, the linear power level was sampled by analog to digital converters covering two ranges: one from 0 to 10% full power and a second from 0 to 150% full power. After scaling, the two readings were merged using equation (5.2.1) before finding the logarithmic power level digitally. A flow diagram is shown in figure (5.2.3).

5.2.2 Error Calculation

The equations for the error, using the zero-order and linearized holds, are given by equations (3.3.1) and (3.3.12) respectively. The first-order hold will be neglected because, from the stability analysis of Chapter 2, it was seen to be the worst of the holds analysed. From equations (3.4.6) and (3.4.8) the demand power level can be given by:

$$\ln N'_d = \ln N_d \left[(n+1)T\right] \qquad (5.2.2)$$

$$= \begin{matrix}\min \\ \max\end{matrix} \left\{ \ln N(nT) \pm C,\ \ln N_d(nT) \pm T/\tau_d,\ \ln N_e \right\} \qquad (5.2.3)$$

where min and + are for power increases and max and - are for power decreases respectively. The last two terms are independent of the sampled

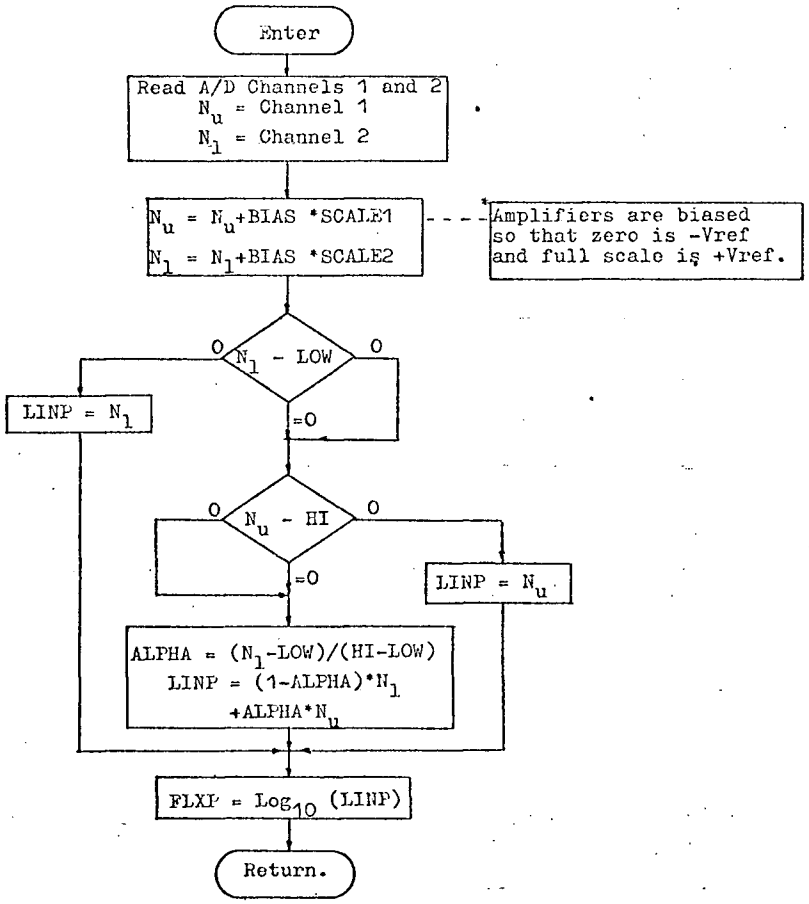

Fig. 5.2.3 Flow Diagram of Neutron Power Fetch

neutron flux and can be calculated and tested before the sampling interrupt (see section 5.2.4). Equation (5.2.3) can then be reduced to

$$\ln N_d\left[(n+1)\ T\right] = \begin{matrix}\min \\ \max\end{matrix} \left\{ \ln N(nT) \pm C,\ \ln N''_d\left[(n+1)T\right] \right\} \qquad (5.2.4)$$

where

$$\ln N''_d\left[(n+1)T\right] = \begin{matrix}\min \\ \max\end{matrix} \left\{ \ln N_d(nT) \pm T/\tau_d,\ \ln N_e \right\} \qquad (5.2.5)$$

A flow diagram of the error calculation is given in figure (5.2.4).

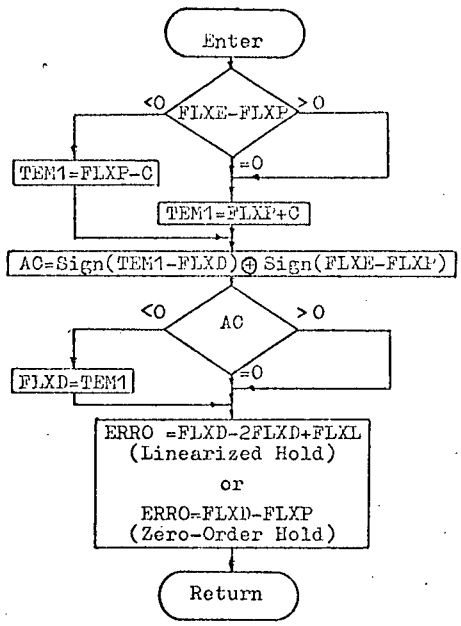

Fig. 5.2.4 Flow Diagram of Error Calculation

5.2.3 Output of Control Action

The precise form of the control action, i.e. moderator level, control rods, depends entirely on the design of the reactor system. However, the input drive in all cases is a velocity signal and the maximum rate of change of reactivity is limited. There are three basic forms of velocity signal:

(a) Bang-bang control with deadband. The reactivity rate is either zero, full speed withdrawal or full speed insertion.

(b) A discrete number of reactivity insertion and withdrawal rates.

(c) A continuously variable reactivity rate, with or without deadband.

The three forms of signal are shown schematically in figure (5.2.5). The most commonly used is the first, due to its simplicity and the low

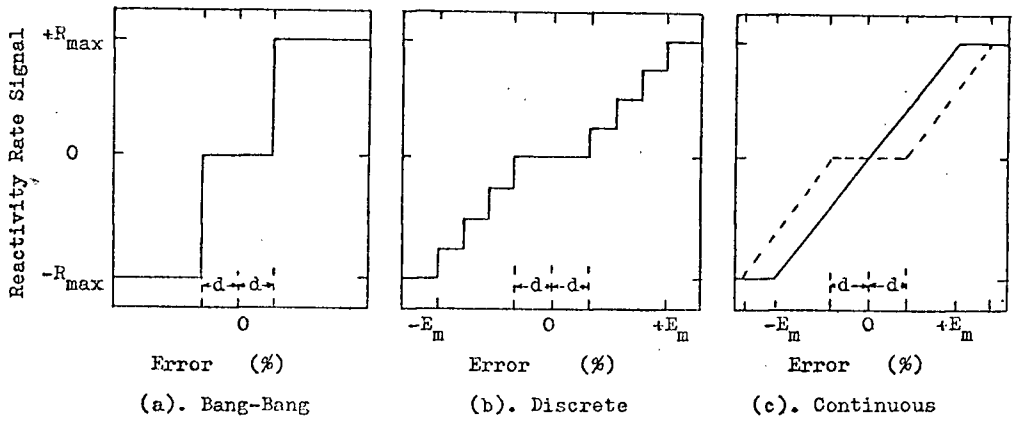

Fig. 5.2.5 Reactivity Rate Signal Types

frequency of rod movement. The discrete system has been limited to two or three reactivity rates, while the continuous systems have always required fairly complex feedback control, i.e. tachometer. With nuclear quality stepping motors now readily available, and coupled with direct digital control, the discrete and continuous systems are now easily realizable without the need for complex feedback systems. Detailed coverage of these systems is given by Schultz[5] and Harrer[15]. Flow diagrams for all three types of system are given in figure (5.2.6). As the maximum reactivity insertion rate for a particular reactor is usually fixed (R_{max}), the stability of the reactor is ensured by choosing the appropriate controller gain (see section 2.6). The variable GAIN sets the required error between the actual neutron power level and the demanded power level to give a maximum reactivity rate signal.

5.2.4 Demand Power Level Calculation

Resides maintaining the reactor on a steady state reactor power, the controller must be able to change the power from one level to another, maintaining the performance within the constraints as given in section 3.1. The linear rate constraint, although applicable only to the higher powered reactors, will be included to give a complete

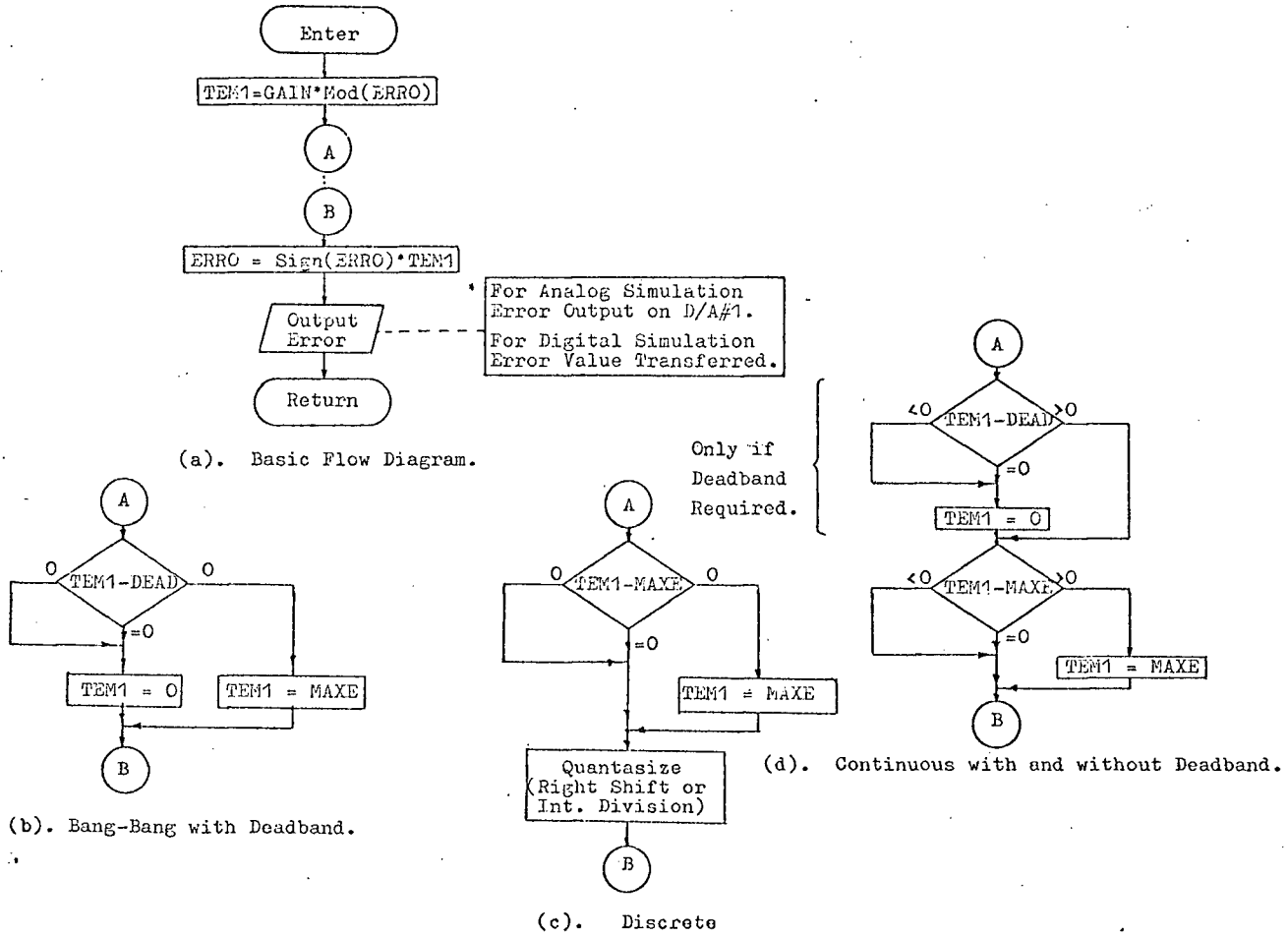

Fig. 5.2.6 Flow Diagram of Control Action Output

general controller. From equation (5.2.3) the demand power level is seen to be a function of the final endpoint and the demanded reactor period. The first term is to ensure that the demand does not diverge too far from the actual power during the initial stages of level changes. Taking the linear rate constraint into account results in the inverse demand period being a function of the power level as given in figure (5.2.7).

Below the switch point S_1 the demand period τ_d is the minimum allowable reactor period τ_m. Above the switch point the inverse demand period is:

$$1/\tau_d = 1/\tau_1 \qquad (5.2.6)$$

$$= \frac{\Delta N}{N_d} \qquad (5.2.7)$$

where

$$\Delta N = \left| \frac{dN}{dt} \right| \max \qquad (5.2.8)$$

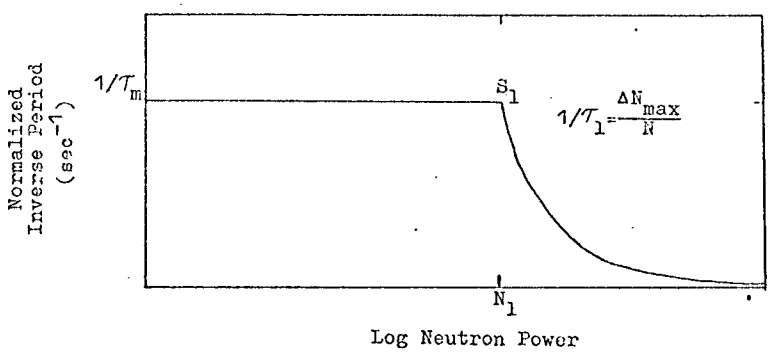

Fig. 5.2.7 Inverse Period for Log and Linear Constraints.

The inverse demand period, besides being physically measurable, is used as it is the form of the period required by equation (5.2.3).

In Chapter 4, dealing with time-optimal control, it was seen that for a power level increase, the control rods are inserted at maximum rate on reaching a switch point S_d until the final demand level is attained. The easiest method is to open the control loop on reaching the switch point, and output a maximum control rod velocity signal, closing the loop again when the final demand power is reached. This method is only suitable under ideal conditions. If, on reaching the switch point S_d, the reactor is rising on a slower period than the minimum allowable period, then with the maximum rate of control rod insertion, the final endpoint will never be reached. The problem as to what control procedure must be followed also arises if the initial power level is above the switch point. With these problems, it is doubtful whether the controller would pass the strict safety regulations with an open loop control band about the final endpoint. The ideal solution is to have dynamic time

optimal control. The study by Lipinski[4] has shown this to be possible, but the complexity of the calculations required after each sampling results in extremely long calculation times, even when a hybrid computer is used.

It was seen in section 4.2 that for a maximum reactivity rate R_{max}, there is a corresponding minimum allowable period τ_e, such that for reactor periods greater than τ_e, no switch point is required. The relationship between R_{max} and τ_e is given by equations (4.2.9) and (4.2.10). Therefore the minimum allowable period at the final endpoint must be greater than τ_e if the neutron power is to be held constant. A possible method of obtaining maximum control velocity, while still maintaining closed loop control, is to increase the demand period to τ_e at the switch point, as in figure (5.2.8). Examination of equation (5.2.3) shows that for power increases the minimum of the three terms is chosen as the demand power level $\ln N_d'$. The neutron power will therefore increase rapidly compared to the demand, with the resulting error giving full control rod velocity. From the error calculation flow diagram (figure 5.2.4), it can be seen that as the neutron power reaches the final endpoint, the demand power $\ln N_d'$ is automatically set to the final endpoint value $\ln N_e$. The disadvantages of this system are that the final endpoint power must be attained, otherwise the demand level $\ln N_d'$ will continue to rise on a period τ_e, instead of being set to the final endpoint. As a result, the neutron power level will turn around and decrease until the demand level is reached, after which the final endpoint will be approached on a period τ_e (see figure (5.2.9)). If the initial power level is above the switch point, then the demand period will be kept constant at τ_e, which is far from optimal.

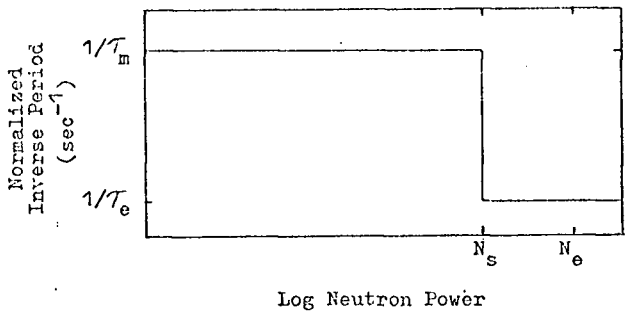

Fig. 5.2.8 Inverse Period for Time Optimal Power Increase. (Step Increase in Period)

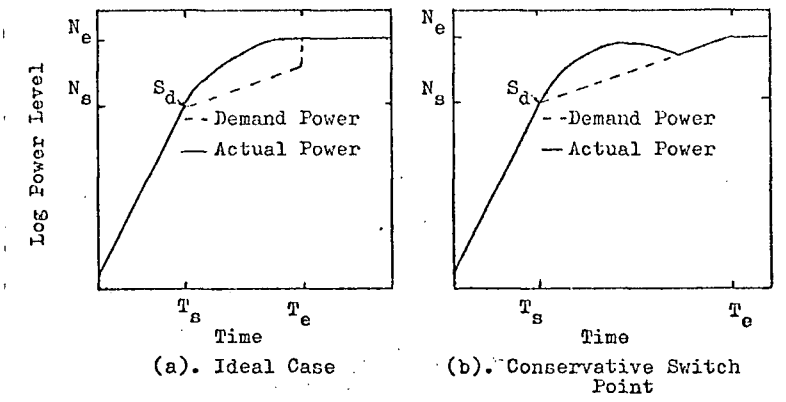

Fig. 5.2.9 Neutron Power Level Increase with Step Period Change

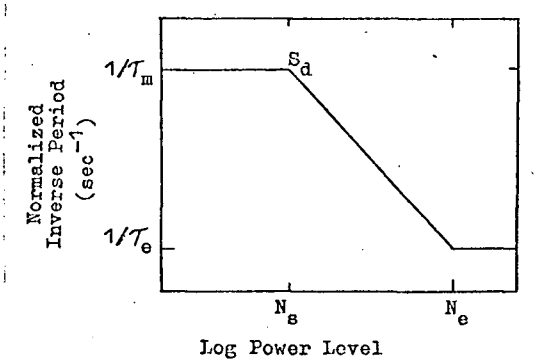

Fig. 5.2.10 Inverse Period for Time Optimal Power Increase. (Continuous Increase of Period)

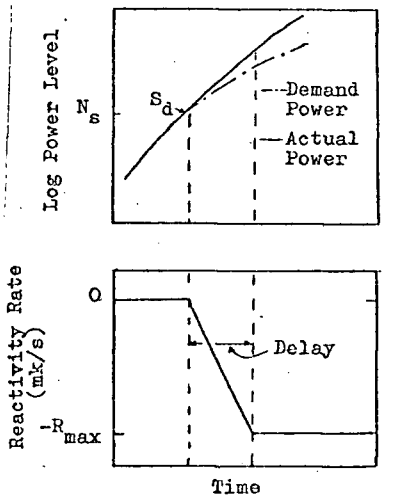

Fig. 5.2.11 Delay in Attaining R_{max} with Continuous Period Increase Case.

If the demand period is gradually increased from τ_m at the switch point to τ_e at the final endpoint as in figure (5.2.10), it should be possible to maintain an error signal giving maximum reactivity rate, while not allowing the demand level to lag too far behind the actual neutron power level, as was the case in figure (5.2.9). This method also permits faster power level changes if the initial level is above the switch point. However, there is now a slight delay after reaching the switch point, before the error is sufficient to output a maximum control signal as shown in figure (5.2.11). This delay is dependent on the controller gain; the higher the gain, the shorter the delay. The switch points given in table 4.2.1 will have to be compensated to make up for the delay. The delay can be shortened by varying the demanded reactor period as shown in figure (5.2.12), as it is often impossible to increase the system gain due to instabilities arising.

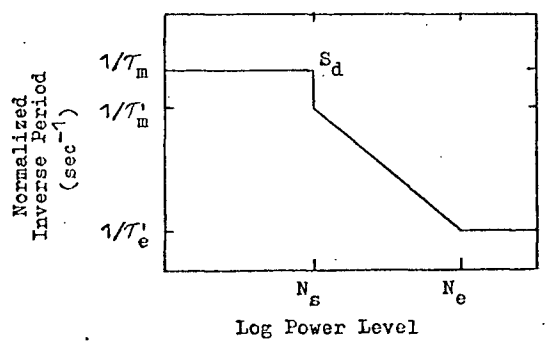

Fig. 5.2.12 Inverse Period for Time Optimal Power Increase. (Continuous plus Step Increase of Period).

Ideally, the demand neutron power should reach the final endpoint at the same instant as the neutron power. The time taken for the demand neutron power level to reach the endpoint from the switch point can be calculated as follows:

Let $L_d = \ln N_d - \ln N_s$

$L_e = \ln N_e - \ln N_s$

$\ln N_d$ = log demand power level

$\ln N_s$ = log switch point power level

$\ln N_e$ = log endpoint power level

τ_m = minimum allowable reactor period

τ_e = allowable reactor period at endpoint

$\Delta = 1/\tau_m - 1/\tau_e$

From figure (5.2.10) it can be seen that for the continuous case

$$L_d(t) = \int_o^t \left\{ 1/\tau_m - \frac{\Delta L_d(t)}{L_e} \right\} \quad dt \qquad (5.2.9)$$

Therefore

$$\frac{dL_d}{dt} = 1/\tau_m - \frac{\Delta L_d}{L_e} \qquad (5.2.10)$$

The solution of this equation is:

$$L_d(t) = L_e/\tau_m \Delta \quad \left[1 - \exp(-t\Delta/L_e)\right] \qquad (5.2.11)$$

The time taken for L_d to reach L_e is required, therefore the following equation is solved for t:

$$t = a\, L_e/\Delta \qquad (5.2.12)$$

where a is solved from

$$\exp(-a) = 1 - \Delta\tau_m \qquad (5.2.13)$$

$$= \tau_m/\tau_e \qquad (5.2.14)$$

For the case where the period is varied as in figure (5.2.12), τ_m is replaced by τ'_m.

The actual times taken by the reactor from the switch point to the endpoint under ideal conditions were measured when the switch points of table 4.2.1 were determined. Table 5.2.1 gives these times for various minimum allowable periods and maximum reactivity rates. The table also gives the times for the demand power level to rise from

the switch point to the endpoint using equations (5.2.12) and (5.2.14). The endpoint period τ_e for the various reactivity rates was determined using equation (4.2.10). It can be seen that, except for those cases

MINIMUM PERIOD (sec).	TIME (SECONDS)							
	R_{max} = .1mk/s		R_{max} = .05mk/s		R_{max} = .02mk/s		R_{max} = .01mk/s	
	Reactor	Demand	Reactor	Demand	Reactor	Demand	Reactor	Demand
20	3.2	2.6	15	13.6	71	75	162	219
30	2.3	.95	11	6.7	50	46.5	121	149
40	1.7	.425	8	3.8	38	31	96	109
50	-	-	5	2.2	29	22	80	84
100	-	-	-	-	11	5.8	37	28.4

Table 5.2.1 Times for Reactor and Demand to Reach Endpoint from Switchpoint

where the maximum reactivity rate is 0.01 mk/second, and where the 20 second period is combined with R_{max} = 0.02 mk/second, the time for the demand power level to reach the endpoint is shorter than that for the reactor. The period can therefore be varied as in figure (5.2.12), to compensate for the delay in attaining a maximum reactivity rate signal. By choosing appropriate values for τ'_m and τ'_e such that:

$$\tau'_m > \tau_m \qquad (5.2.15)$$

and

$$\tau'_e \geq \tau_e \quad , \qquad (5.2.16)$$

the reactor and demand power levels can reach the final endpoint at the same instant. Table 5.2.2 gives values for τ'_m and τ'_e using the switch points of table 4.2.1.

The problem still exists for those cases where the demand power level takes longer than the reactor to reach the endpoint. If a slightly shorter value for τ_e can be tolerated, the time for the demand to reach

the endpoint can be made the same as the reactor. The appropriate values of τ'_e were included in table 5.2.2. Whether these values can be tolerated will be determined when the controller is tested in section 5.5.

The preceding analysis has been for power increases. Similarly, for power level decreases the same procedure can be followed, with the reactor period varied as in figure (5.2.13). Table 5.2.3 gives the switch point values, the time for the reactor to reach the endpoint and appropriate values of τ'_m and τ'_e.

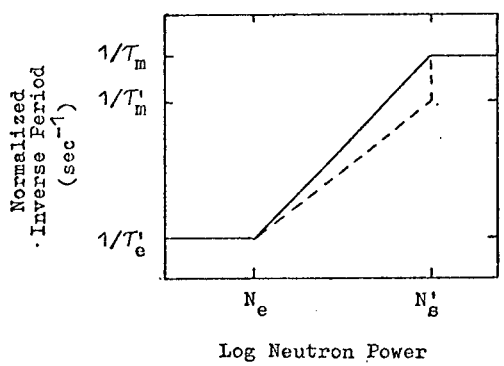

Fig. 5.2.13 Inverse Period for Power Level Decrease . (Continuous Increase of Period).

MINIMUM PERIOD (sec).	τ'_m and τ'_e (sec)							
	R_{max} = .1mk/s		R_{max} = .05mk/s		R_{max} = .02mk/s		R_{max} = .01mk/s	
	τ'_m	τ'_e	τ'_m	τ'_e	τ'_m	τ'_e	τ'_m	τ'_e
20	30	51	25	110	24	180	24	165
30	94*	94*	67	115	35	280	35	245
40	182*	182*	137*	137*	56	307	46	315
50	-	-	167*	167*	75	307	57	465
100	-	-	-	-	314*	314*	151	627

*Note: $\Delta = 0$, therefore $\tau'_m = \tau'_e = L_e/t$

Table 5.2.2 τ'_m and τ'_e for Simultaneous Arrival of Reactor and Demand at Endpoint

R_{max} mk/sec	Switch Point N_s/N_e	Time to Endpoint (sec)	τ'_m (sec)	τ'_e (sec)
.05	1.008	1.9	211	211
.02	1.188	37	150	310
.01	1.63	114	140	475

Table 5.2.3 Parameters for Power Decreases with 100 second Minimum Period Constraint

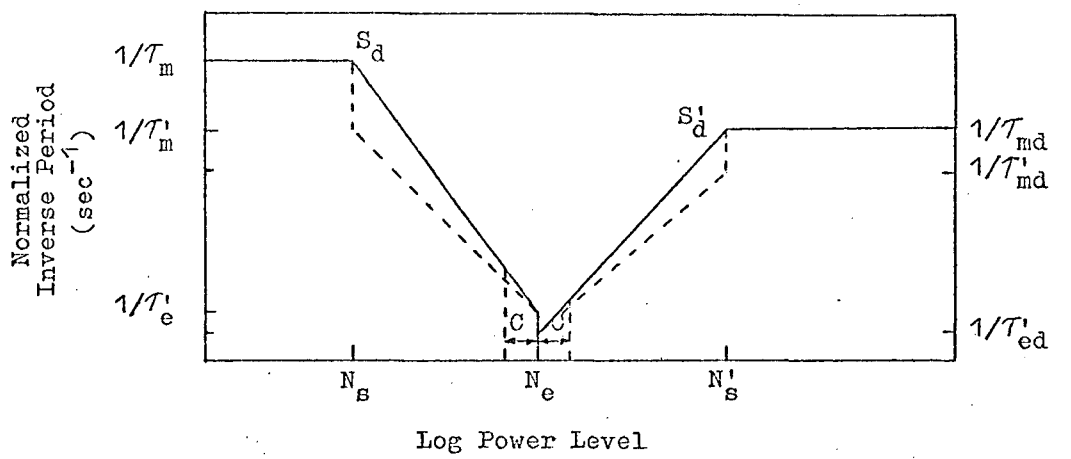

Fig. 5.2.14 Inverse Period as a Function of Power Level

If the reactor is at steady state, the variation of the demand period about the steady state level is given in figure (5.2.14). There is a deadband of value C on either side of the steady state level and if the neutron power level remains in this deadband, the demand power level is held at the steady state level. If the neutron power level should deviate outside the deadband the demand power level $\ln N_d'$ is set to the value $\ln N \pm C$, depending on whether it is below or above the steady state. (See the error flow diagram of figure (5.2.4)). The demand power level $\ln N_d'$ is then returned to the steady state level with the demand period varying as in figure (5.2.14). Figure (5.2.15) shows the variation of the demand period when the final endpoint is in the range where the linear rate constraint is active.

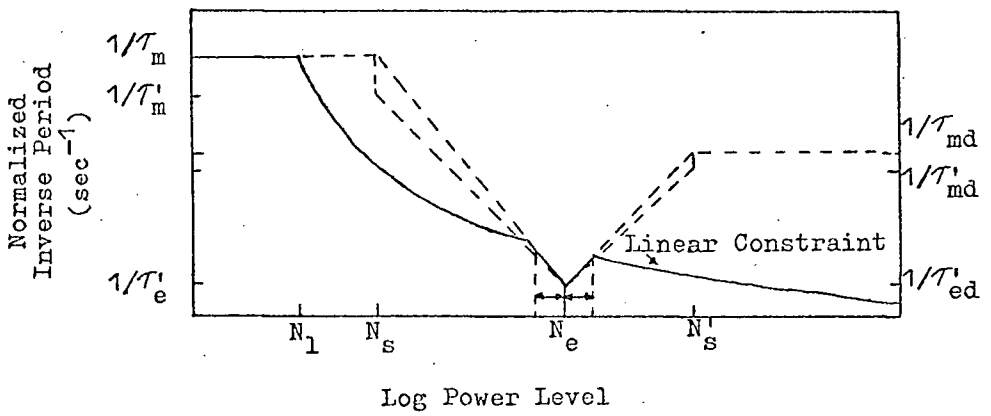

Fig. 5.2.15 Inverse Period as a Function of Power Level (Linear Constraint)

A flow diagram of the demand power level calculation is given in figure (5.2.16). It must be remembered that the switch points given in table 4.2.1 are for ideal conditions. If there is any delay in attaining a maximum reactivity rate signal after the switch point, the switch point must be compensated to avoid over- or undershoot of the final level.

It is probable that the controller developed will have a sub-optimal response. Just how sub-optimal it is, will be determined in subsection 5.5, where the controller is tested using a digital simulation of a thermal reactor. The results obtained for power level increases and decreases will be compared to the ideal results of Chapter 4 and necessary adjustments in the switch points will be determined.

5.2.5 New Endpoint and Switch Point Calculations

The only probable interaction between the safety system and the controller would be the setting of the final endpoint by the safety system for controlled power reversals and power level limit setbacks. Program or operator initiated power level holds can also be expected. A logic diagram of possible endpoint priorities is given in figure (5.2.17). The switch points associated with a particular endpoint are

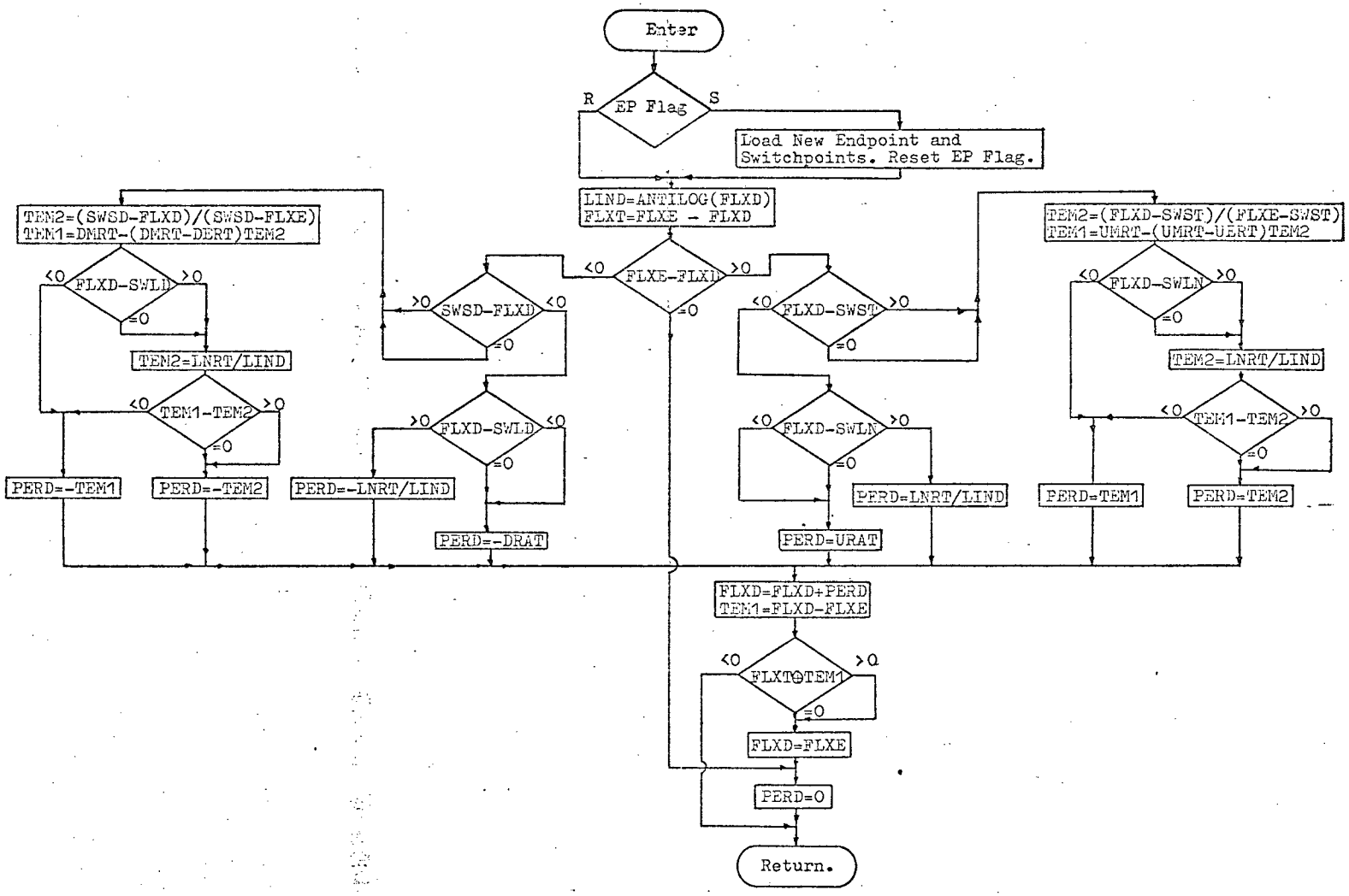

Fig. 5.2.16 Flow Diagram of Demand Calculation

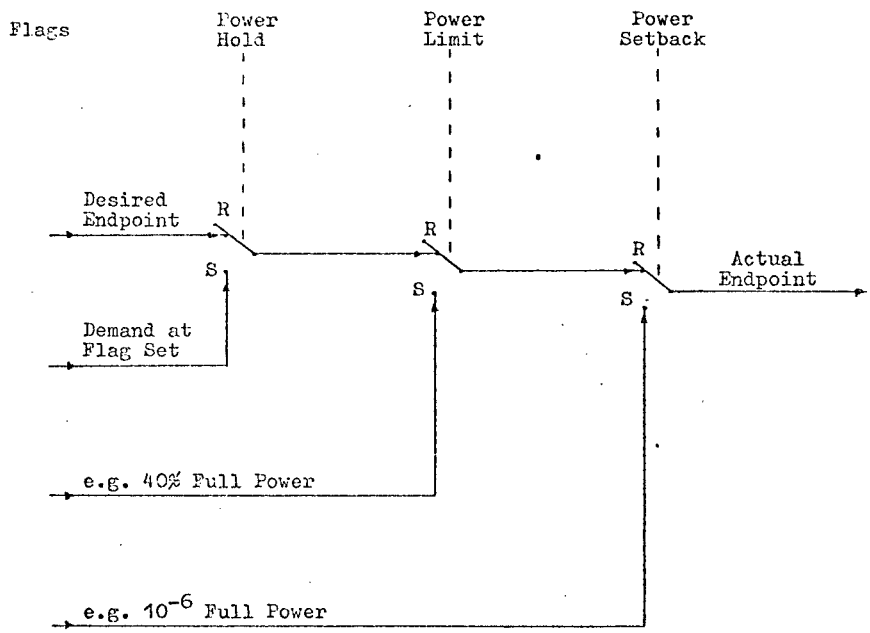

Fig. 5.2.17 Endpoint Priority Chain

simple to calculate. As the maximum reactivity rate R_{max} and the minimum allowable reactor period τ_m are fixed for a reactor, the switch points for time optimal control for a particular endpoint N'_e are given as follows:

$$\ln N_{si} = \ln N'_e + \ln S_{di} \qquad (5.2.9)$$

where i = 1 is for power increases

i = 2 is for power decreases

and S_d = ratio of N_s/N_e as determined by simulation methods described in Chapter 4.

The linear rate switch point remains fixed, independent of the final endpoint and is given by

$$N_1 = \tau_m \left|dn/dt\right|_{max} \qquad (5.2.10)$$

With the occurrence of a reactor scram or emergency shutdown, the endpoint is set to the minimum power level, the controller output disconnected and the demand power level allowed to float down with the neutron power level.

5.2.6 General Remarks

Throughout the development of the controller, an attempt was made to minimize the calculation time from the sample interrupt to the output of the control action. All calculations not dependent on the measured neutron flux, were completed prior to the sample interrupt. The algorithm as it stands is by no means complete. Areas such as shim and regulator rod control, maintaining the regulator rod at maximum effectiveness and many others have not been included as in most cases they are dependent on the individual reactor type.

From the stability analysis of Chapter 2, it was seen that except for extremely fast sampling rates, the zero-order hold was the best of the three hold types. Examination of equation (3.3.1) shows that at steady state there is only proportional control, with no rate control. If the error equation (3.3.12) for the linearized hold is broken down, the following form can be obtained:

$$\varepsilon_n(t) = [\ln N_d(nT) - \ln N(nT)] + \left\{ T/\tau_d - [\ln N(nT) - \ln N(n-1)T] \right\} \qquad (5.2.11)$$

Therefore, it can be seen that the linearized hold gives proportional plus rate control.

5.3 Digital Simulation of a Nuclear Reactor

The controller requires as input a logarithmic neutron power level and outputs control action in the form of a limited reactivity rate signal.

The point reactor kinetics equations with six groups of delayed neutrons are given in Appendix A by equations (A.1.1) and (A.1.2). These equations result in a linear neutron power. Dividing through by n in both

equations gives:

$$\frac{dn}{dt} / n = \frac{\delta k}{\ell} - \frac{\beta}{\ell} + \sum_{i=1}^{6} \lambda_i C_i/n + S/n \qquad (5.3.1)$$

and

$$\frac{dC_i}{dt} /n = \frac{\beta_i}{\ell} - \lambda_i C_i/n \qquad (5.3.2)$$

Let

$$m = \frac{dn}{dt} / n \qquad (5.3.3)$$

$$V_i = C_i/n \qquad (5.3.4)$$

and

$$w = S/n \qquad (5.3.5)$$

Substitution into equations (5.3.1) and (5.3.2) gives

$$m = \frac{\delta k}{\ell} - \frac{\beta}{\ell} + \sum_{i=1}^{6} \lambda_i V_i + w \qquad (5.3.6)$$

and

$$\frac{dV_i}{dt} = \frac{\beta_i}{\ell} - V_i (m + \lambda_i) \qquad (5.3.7)$$

The quantity $\frac{dn}{dt} / n$ is the inverse reactor period. Also

$$\log_e n = \int m \, dt \qquad (5.3.8)$$

Therefore with the change in the variable, the logarithmic neutron power can be obtained directly from the simulation, with the simulation input of reactivity being retained. Equations (5.3.6) to (5.3.8) are more suited to digital than to analog simulation techniques. The six equations of the form of (5.3.7) require extremely accurate and relatively fast multipliers which are not always available. The main problem is the "open loop" integrator of equation (5.3.8). Both of these problems are elimi-

nated with digital simulation techniques. The change in variable has the added advantage of normalizing the equations, with the delayed neutron precursors being transferred into ratios instead of absolute values extending over the range of power level of a nuclear reactor. It is therefore possible to use the fixed point arithmetic routines developed for the controller, with much faster calculation times possible than would be the case with floating point arithmetic.

Much criticism has been levelled at digital simulation techniques due to the inherent quantization and serial operation. Many sophisticated methods for the numerical solution of differential equations have been proposed in an attempt to reduce the errors incurred by digital techniques. One of the so-called "unsophisticated" integration methods, the trapezoidal integration method, was used in the digital simulation of the nuclear reactor because of its simplicity, ease of programming and excellent stability properties[28]. The form of trapezoidal integration is as follows:

$$y_{n+1} = y_n + \frac{3T}{2} f_n - \frac{T}{2} f_{n-1} \qquad (5.3.9)$$

where

y_n = the output of the integrator at time nT

f_n = sum of inputs to the integrator at time nT

and T = sample period.

The accuracy of the digital simulation as a function of sample period T was tested against the analog simulation described in section 5.5 for step inputs in reactivity. With a sample period of 0.1 second, there was a noticeable error in the order of 5% during the initial stages after the step where the influence of the prompt neutrons was the greatest. With a 0.05 second sample period, this error was reduced to 1%, while at

a sample period of 0.01 second, the error could not be distinguished in the noise of the analog computer simulation. For the longer sample periods, the error was only detectable in the initial stages where the prompt neutrons were effective. Although the simulation was accurate when the effect of the delayed neutrons became prominent, the initial error was carried forward and remained.

A flow diagram of the basic digital simulation is given in figure (5.3.1). Using a sample period of 0.01 second, the simulation

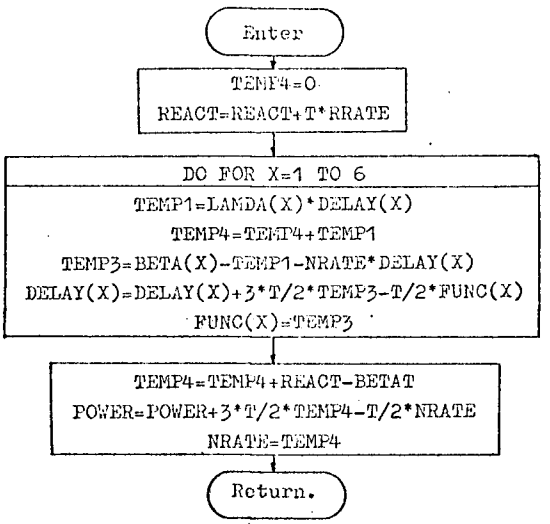

Fig. 5.3.1 Digital Simulation of Nuclear Reactor-
Flow Diagram. (One Sampling Only)

time was about half the real time. A handler was developed to control the digital simulation and controller and pass the necessary variables between the two programs. The handler provides on line graphic readout of the logarithmic power level, reactor period, reactivity rate and total reactivity, and also prints out final results on a strip chart recorder. Program interruption and re-initialization or the setting of any variable is possible without disturbing the continuous simulation sequence. The three sample periods, simulation, controller and readout are independent of each other and can be set to the required values. The handler simu-

lated the neutron power measuring circuits (see section 2.5) by averaging the neutron power from one controller sampling to the next, before passing the neutron power level to the controller.

A thermal reactor with parameters as given in Appendix A.4 was simulated for the testing of the digital controller.

5.4 Analog Simulation of a Nuclear Reactor

The point kinetics equations with six groups of delayed neutrons are given in Appendix A by equations (A.1.1) and (A.1.2). The analog computer circuit diagram is given in figure (5.4.1). The analog simulation was set up on an EAI, PACE 231R analog computer which is interfaced to the PDP-9 computer used for the digital controller.

The neutron power level measuring circuit described in section 2.5 is simulated by integrating the neutron power level from one sampling to the next and by initializing the integrator after each sampling. Fortunately the 231R analog computer is equipped with electronic switching for the integrator modes and the shorter sample periods of 0.1 second can be easily handled. Two measuring ranges are used; one up to 10% and the second to 150% full power. The two ranges are merged using the technique described in section (5.2.1). The outputs of the two integrators are sampled by a multiplexed analog to digital converter. No timing problems were encountered as all the inputs to the multiplexer are preceded by sample and hold units and the integrators are initialized immediately after sampling and holding the two signals. The initial conditions of the two integrators are biased, so as to allow full use of the A/D sampling range of $\pm$ Vref, thereby gaining double the number of digitized power levels.

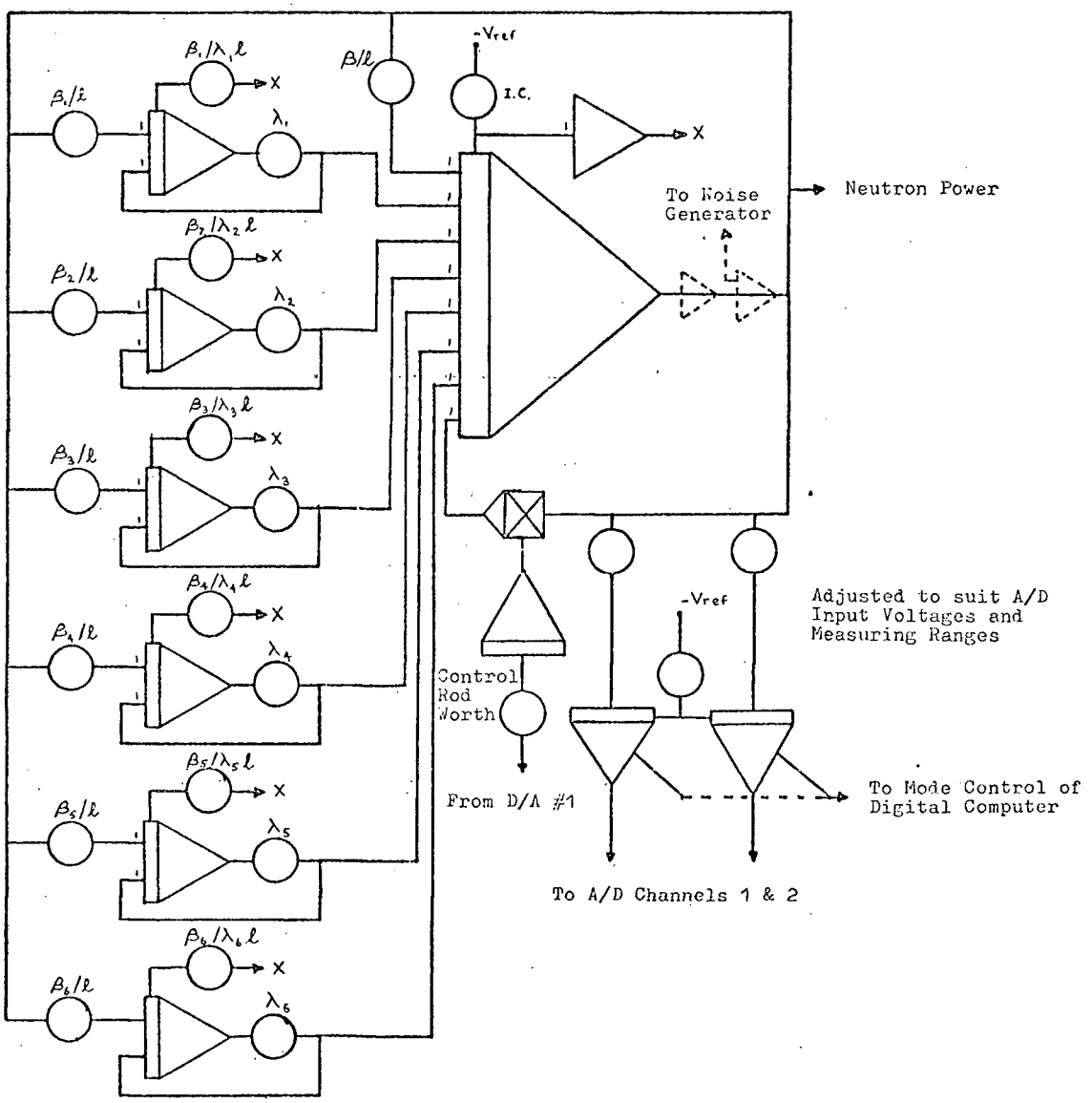

Fig. 5.4.1 Analog Simulation of Nuclear Reactor

The control action in the form of a reactivity rate or a total reactivity signal is returned to the analog simulation from the controller by means of a digital to analog converter.

The same reactor parameters were used as for the digital simulation. (See Appendix A.4).

5.5 Test of Digital Controller

Both analog and digital simulations described in the previous

subsections will be used in testing the digital controller. The advantage of the digital simulation is that it covers the entire range of possible reactor power levels. Another advantage is that no additional external equipment is necessary for the testing of the digital controller. The analog computer simulation provides the best real time conditions with the monitoring and calculation delays, as would be expected in an actual reactor system. The disadvantage is that the range is limited to about 2 decades of operation. Automatic rescaling is possible with powerful and advanced analog systems, but they are not always available.

5.5.1 Calculation Time of Control Algorithm

Using the analog simulation, the time taken from the moment the sampling of the neutron power is begun, to the output of the control action is 0.8-1.1 ms. More than half of this time is required in the sampling, merging and finding the logarithm of the neutron power. These problems encountered using a "hybrid" simulation are the same as would be encountered in a true on-line system. The longer calculation times of 1.1 ms are required when two measuring ranges are merged. The total time from the sampling to the exit after calculating the next demand level is 1.5 - 1.8 ms. Even with the shortest sample period of 0.1 second, the effect of the calculation delay before the output of the control action can be neglected. The use of the logarithmic control algorithm and fixed point arithmetic can be seen to give exceptionally fast and simple calculations. The time taken from sampling to the output of control action is about twice as long as the time for an addition using the computer's floating point package.

5.5.2 Stability Test of Controller

The overall system stability was analysed in section 2.6. For

a particular sample period T, the stability of the reactor could be ensured by maintaining the reactivity rate per unit error less than a maximum value R_{max}. Table 2.6.1 gives R_{max} per unit error for various sample periods for the thermal reactor of the analog and digital simulations.

The most convenient method of testing the overall stability is to use the analog simulation. By means of adjusting the control rod gain potentiometer, the gain can be increased slowly until stability is lost. For both the linearized and zero-order holds, the values given in table 2.6.1 were conservative. The value of R_{max}, where stability was lost, was 25 to 35% greater than the theoretical values for all four sample periods. This is an ideal situation from the safety point of view, as the theoretical calculations of section 2.6 then have a safe 25% margin. When using the digital simulation, the results differed by no more than 2% from those obtained using the analog simulation.

5.5.3 Power Level Increases

Using the digital simulation, the controller was tested for power increases using the switch points of table 2.6.1 and the respective values of τ'_m and τ'_e as in table 5.2.2. A sample period of 0.1 second was used throughout the testing, as one of the main reasons for the logarithmic control algorithm was to allow the use of these fast sample frequencies.

Figure (5.5.1) shows power increases with a 20 second minimum allowable period and a maximum reactivity rate of 0.02 mk/second. With the controller gain such that a .1%/decade error between the power level and the demand gave a maximum reactivity rate signal, the overshoot was never more than 0.5% of the final endpoint, for all the combinations

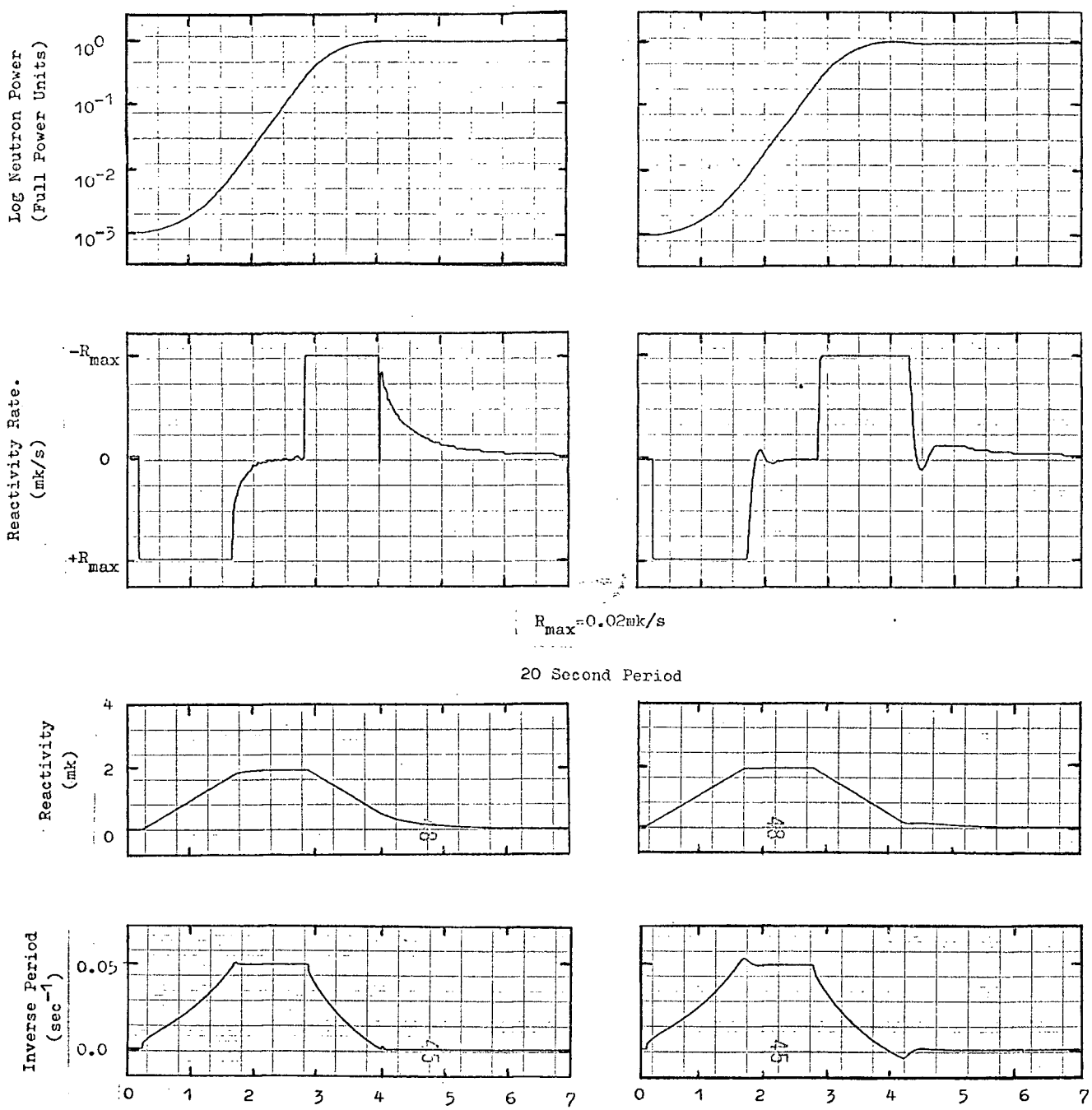

(a). 0.1%/Decade Error = R_{max} Output

(b). 1%/Decade Error = R_{max} Output

Fig. 5.5.1 Time Optimal Power Increase

of period and R_{max} given in table 2.6.1. When using a lower controller gain, such that an error of 1%/decade resulted in R_{max} out, the overshoot in all cases was between 5 and 7% of the final endpoint. This greater overshoot is not only due to the delay in attaining a maximum reactivity signal but also because an overshoot of 2.3% of the final endpoint is required to obtain a maximum output signal. These results are excellent, with the overshoot being a little over twice the error required for a maximum reactivity signal.

Examination of figure (5.5.1) shows that the period becomes shorter than the minimum allowed just prior to attaining an asymptotic period. During the initial stages of start-up, the demand does not deviate too far from the power level, due to the first term of equation (3.4.6). This peak in the inverse period occurs as the power finally catches up with the demand. The amount of peaking can be reduced by reducing C of equation (3.4.6). The most suitable value of C was found to be in the order of one-and-one-half times to twice the error required for a maximum reactivity signal.

In tables 5.2.1 and 5.2.2, it was seen that for the smaller values of R_{max}, τ'_e had to be smaller than the desired final endpoint period τ_e, so that the demand and power levels reached the endpoint together. To see whether these values of τ'_e could be tolerated, the reactor was set on a power increase with a minimum allowable period of τ'_e. On attaining an asymptotic period, the control rods were inserted at maximum velocity and the overshoot measured. For the case of τ'_e = 165 seconds, (instead of the desired 627 seconds) and R_{max} = 0.01 mk/second, the overshoot was 6.5%. With a τ'_e of 245 seconds, this overshoot reduced to 2.5%. These overshoots were much less than those obtained when

there was a sizable delay in attaining a maximum reactivity rate signal after the switch point. Fortunately, the probability of any reactor having a 20 second allowable period is small, especially if it only has a reactivity rate of 0.01 mk/second and the values of τ_e can therefore be tolerated where necessary. The greater overshoot will only be found in those cases where: (a) the switch point is conservative, (b) the minimum allowable period has not been attained and (c) the initial power level is above the switch point, all of which are shown in figure (5.5.2).

As was expected, the controller is suboptimal. However, the higher the controller gain, the closer to the ideal is the performance. Taking as examples the cases shown in figure (5.5.1), the ideal time from switch point to endpoint is 71 seconds. With a controller gain of .1%/decade for an output of R_{max}, the time for the power finally to settle within .23% of the endpoint is 71.5 seconds. When the gain is 1%/decade, the corresponding time to settle within 2.3% of the endpoint is 86 seconds. This longer time is due to the greater overshoot, which is a direct result of the delay in attaining a maximum reactivity signal. For these lower gain cases, the time could be shortened slightly by making the logarithmic switch point conservative by about 2% of a decade. It can be seen in figure (5.5.1(a)) from the spike in the reactivity rate signal, how the demand and reactor power reach the endpoint simultaneously, followed by an instantaneous maximum signal which tapers off while precursor density equilibrium is attained.

Figure (5.5.3) shows a power increase when a linear rate constraint of 1% full power per second is imposed. The reactor is first constrained by the minimum allowable period, followed by the linear rate constraint and finally the time optimal constraint.

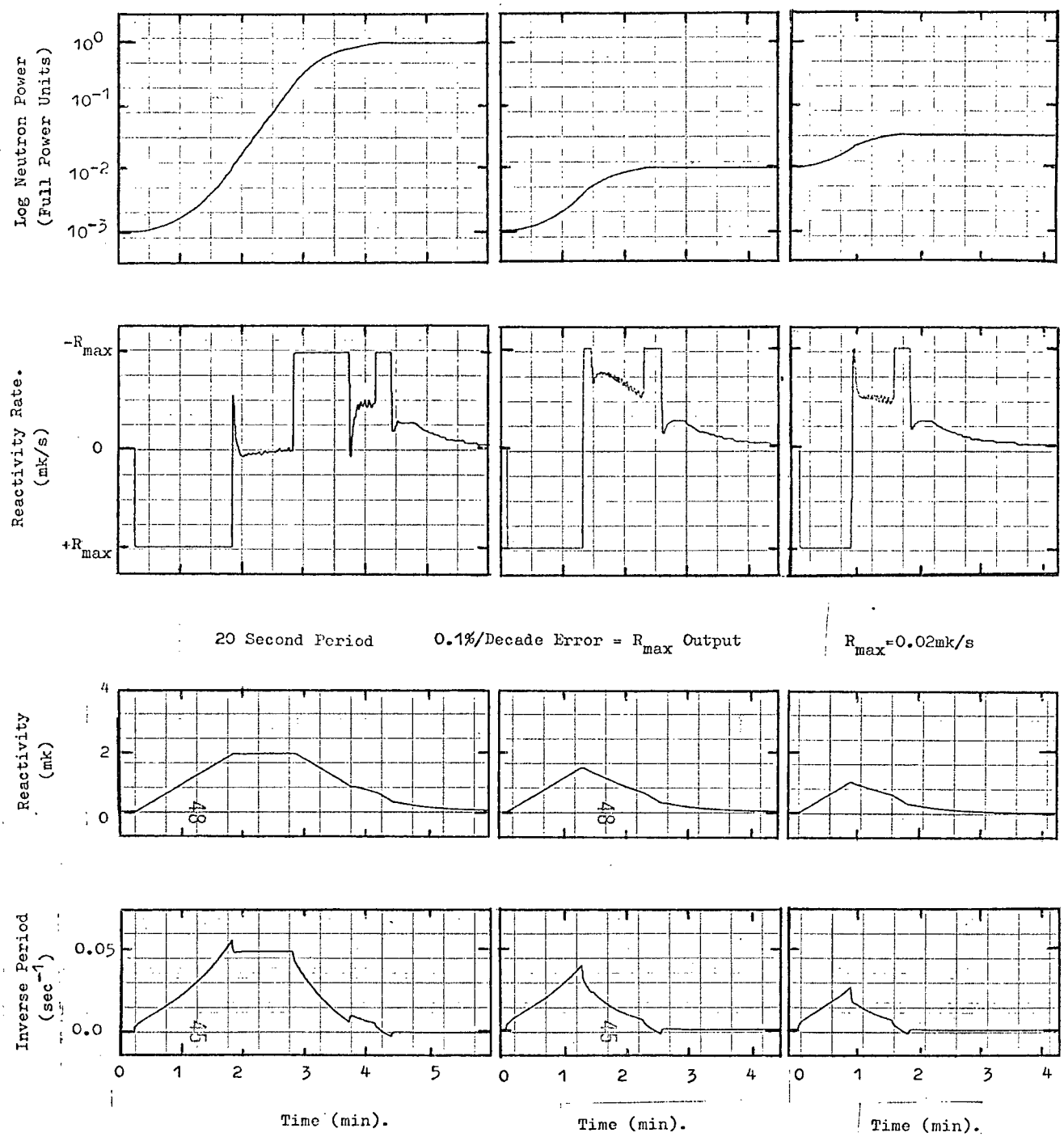

(a). Conservative Switch Point.

(b). Period Longer Than Demand Period on Reaching Switch Point.

(c). Intial Power Level Above Switch Point.

Fig. 5.5.2 Power Level Increases

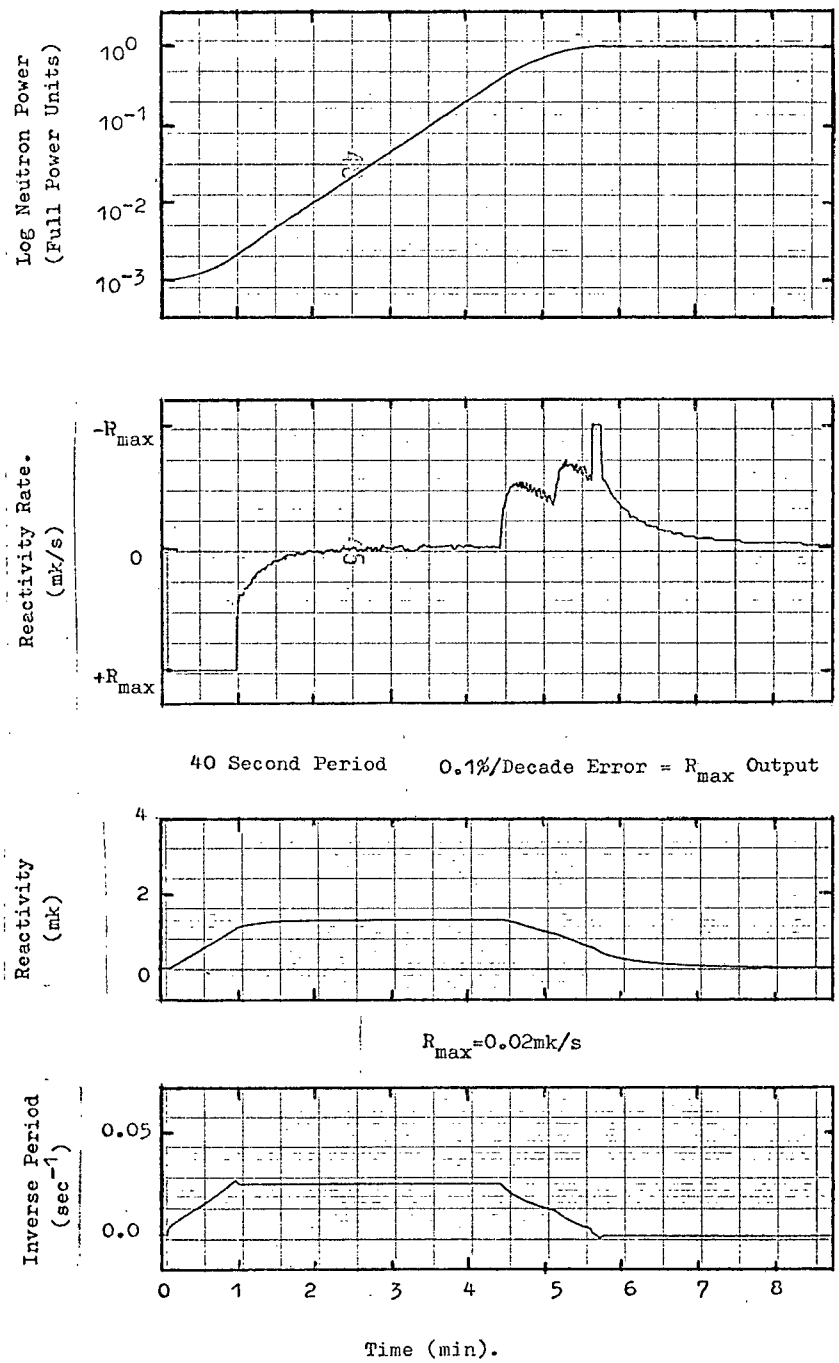

Fig. 5.5.3 Power Level Increase with Linear Rate Constraint

5.5.4 Power Level Increases with Noisy Reactor

The analog simulation was used for testing the controller with a noisy reactor. This made it easy to add various noise signals; furthermore, the simulation included the digitizing effect of the analog to digital converters. Figure (5.5.4) shows a power increase with a white noise signal with R.M.S. value of 3% of full power. The overshoot of the final endpoint was only .5% greater than the reactor without noise. Removal of the filtering circuit before the A/D converter resulted in much poorer performance, especially at low power, due to the low signal to noise ratio.

A linear power signal is read by the A/D converters and the logarithmic power is digitally calculated. The resulting uneven spread of digitized power levels can be clearly seen in the reactivity rate signal of figure (5.5.4). As stated previously, the use of logarithmic ion chamber amplifiers will alleviate this problem.

5.5.5 Power Level Decreases

A power level decrease with a 100 second period constraint is shown in figure (5.5.5). The undershoot was found to be twice the error required for a maximum output signal, which was identical to the results for power increases. As mentioned in section 4.3, time optimal power decreases were not dealt with due to the wealth of existing literature.

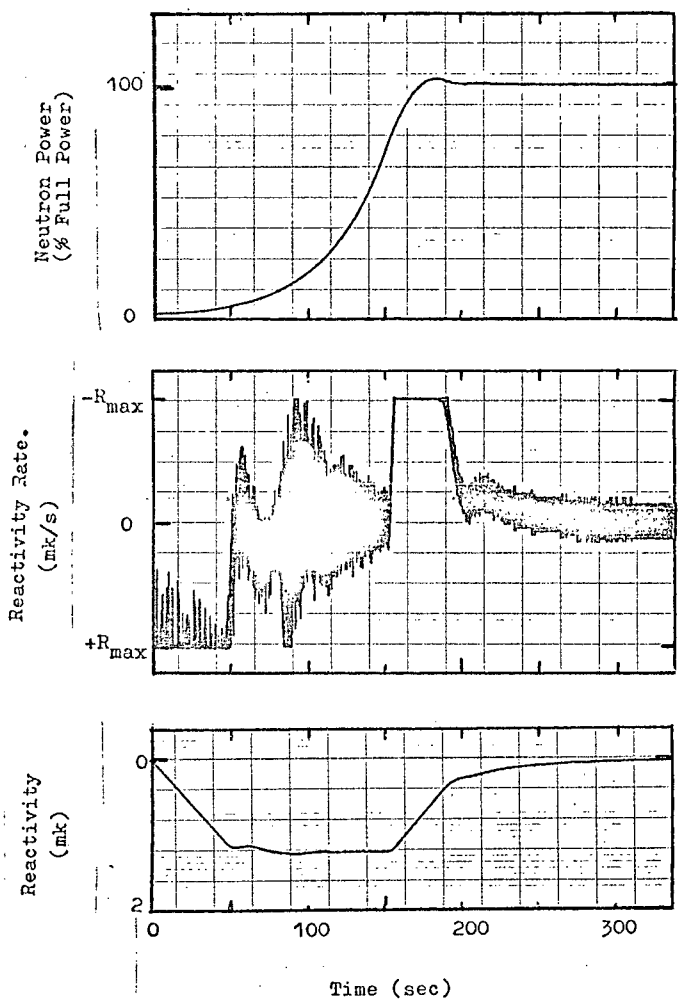

Fig. 5.5.4 Power Level Increase with Noisy Reactor

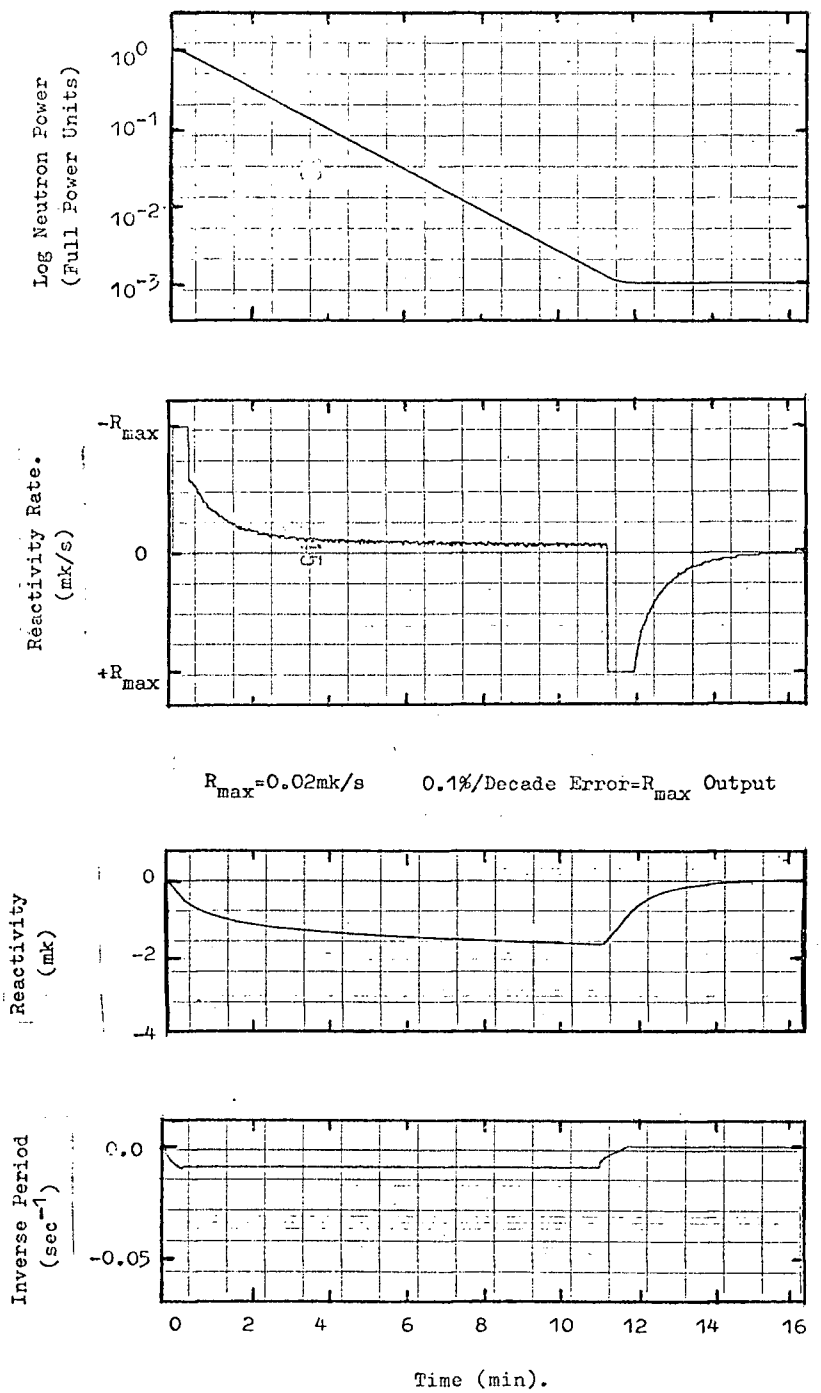

Fig. 5.5.5 Power Level Decrease with 100 Second Period

6. CONCLUSIONS

A basic error sampled data control system for a nuclear reactor was developed. The control system was analysed for stability with various sampled data holds and sample frequencies. The results obtained, when compared to those measured with digital and analog simulations, proved safe, with a 25% margin.

A digital control algorithm, using the logarithmic neutron power level as input, was developed, which allowed the use of fixed point arithmetic. The calculation speeds of the algorithm were seen to be much faster than algorithms using floating point arithmetic. Time optimal power increases were studied, and a time optimal control sequence using switch points was derived. The determination of the switch points was done by simulation techniques, eliminating the use of complex and very approximate calculations.

A practical demand power level controller was developed, using machine language programming. All calculations not requiring the sampled neutron flux were calculated prior to the sample interrupt, in an attempt to minimize the delay from the sampling to the output of control action. The actual delay was found to be from 0.8 to 1.1 ms, which is the time required for approximately two floating point additions. Time optimal power increases were tested using a digital simulation of a thermal reactor. The overshoot of the final endpoint was seen to be twice the error required for a maximum reactivity rate signal which is most satisfactory. The controller, although sub-optimal, approached the ideal time optimal trajectory as the controller gain was increased. A controller gain of .1%/decade for a maximum reactivity rate signal resulted in near time-optimal results.

It can be concluded that a successful, near time-optimal control algorithm has been developed with general applications to low power reactors.

APPENDIX A. REACTOR KINETICS EQUATIONS

A.1 General Reactor Kinetics Equations

The space independent reactor kinetics equations for six groups of delayed neutrons are[5]:

$$\frac{dn}{dt} = \frac{\delta k - \beta}{\ell} n + \sum_{i=1}^{6} \lambda_i C_i + S \qquad (A.1.1)$$

and

$$\frac{dC_i}{dt} = \frac{\beta_i}{\ell} n - \lambda_i C_i \qquad (A.1.2)$$

where

n = neutron density (neutrons/cm^3)

β = total fraction of delayed neutrons

δk = reactivity

ℓ = mean effective lifetime of a neutron (sec)

C_i = concentration of neutrons in the ith delayed group (neutrons/cm^3)

λ_i = decay constant of the ith delayed group (sec^{-1})

β_i = fraction of neutrons in the ith delayed group

S = source strength (neutrons/cm^3/sec)

The space independent reactor kinetics equations in the absence of an external source for one group of delayed neutrons are[5]:

$$\frac{dn}{dt} = \frac{\delta k - \beta}{\ell} n + \lambda C \qquad (A.1.3)$$

and

$$\frac{dC}{dt} = \frac{\beta}{\ell} n - \lambda C \qquad (A.1.4)$$

where

$$\lambda = \beta \Big/ \sum_{i=1}^{6} \beta_i / \lambda_i \qquad (A.1.5)$$

A.2 Linearized Reactor Kinetics Equations

Linearized kinetics equations about a power level n_o are as follows[5]:

$$\frac{dn}{dt} = -\frac{\beta}{\ell} n + \sum_{i=1}^{6} \lambda_i C_i + S + \frac{\delta k}{\ell} n_o \qquad (A.2.1)$$

and

$$\frac{dC_i}{dt} = \frac{\beta_i}{\ell} n - \lambda_i C_i \qquad (A.2.2)$$

For the single delayed group model the linearized kinetics equations in the the absence of an external source are[5]:

$$\frac{dn}{dt} = -\frac{\beta}{\ell} n + \lambda C + \frac{\delta k}{\ell} n_o \qquad (A.2.3)$$

and

$$\frac{dC}{dt} = \frac{\beta}{\ell} n - \lambda C \qquad (A.2.4)$$

A.3 Reactor Kinetics Transfer Function

Using the linearized kinetics equations the reactor transfer function is as follows[2,4]:

$$\frac{N(s)}{n_o k(s)} = 1 \Big/ \left\{ \ell s + \beta + \sum_{i=1}^{6} \lambda_i \beta_i / \left[s + \lambda_i \right] \right\} , \qquad (A.3.1)$$

The transfer function for the one delayed group model is:

$$\frac{N(s)}{n_o k(s)} = \frac{s + \lambda}{\ell s (s + \lambda + \beta/\ell)} \qquad (A.3.2)$$

A.4 Thermal Reactor Parameters

The parameters of the delayed neutron groups of the thermal reactor used throughout this study are given in table A.4. The total fraction of delayed neutrons is:

$$\beta = 0.0064$$

the mean effective neutron lifetime is:

$$\ell = 10^{-3} \text{ sec}$$

From equation (A.1.5) the decay constant for the single delayed neutron group case is:

$$\lambda = 0.076 \text{ sec}^{-1}$$

Group Number i	Decay Constant λ_i (sec^{-1})	Fraction of Delayed Neutrons β_i
1	0.0124	0.00024
2	0.0305	0.00140
3	0.1110	0.00125
4	0.3010	0.00253
5	1.1400	0.00074
6	3.0100	0.00027

Table A.4 Parameters of Delayed Neutron Groups of a Thermal Reactor

REFERENCES

1. Pearson, A., "The Future of the Digital Computer in Power Reactor Instrumentation", Trans. Am. Nucl. Soc., 9, 266, 1966.

2. Marciniak, T.J., "Time-Optimal Digital Control of Zero-Power Nuclear Reactors", ANL-7510, October 1968.

3. Cohn, C.E., "Further Use of an On-Line Computer in Reactor Physics Experiments", Trans. Am. Nucl. Soc., 9, 262, 1966.

4. Lipinski, W.C., "Optimal Digital Computer Control of Nuclear Reactors", ANL-7530, January 1969.

5. Schultz, M.A., "Control of Nuclear Reactors and Power Plants", 2nd ed., McGraw-Hill Book Co., New York 1961.

6. Tou, J.T., "Digital and Sampled-Data Control Systems", McGraw-Hill Book Co., New York, 1959.

7. Hafner, W.L., "All Roots of Polynomial Equations with Real Coefficients", ANL-C252, March 1966.

8. Pearson, A., Lennox, C.G., "Sensing and Control Instrumentation", "The Technology of Nuclear Reactor Safety", Volume 1, Eds. Thompson and Beckerley, The M.I.T. Press, Cambridge, Massachusetts, 1964.

9. Cohn, C.E., "Speed Tests on Some Control Computers", Trans. Am. Nucl. Soc., 13, 177, 1970.

10. Pontryagin, L.S., et al., "The Mathematical Theory of Optimal Processes", Interscience Publishers, New York, 1962.

11. Bellman, R., "Adaptive Control Processes", Princeton University Press, 1961.

12. Monta, K., "Time Optimal Digital Computer Control of Nuclear Reactors, (I):- Continuous Time System", J. Nucl. Sci. Technol. 3(6), 227, June 1966.

13. Monta, K., "Time Optimal Digital Computer Control of Nuclear Reactors, (II):- Discrete Time System", J. Nucl. Sci. Technol., 3(10), 419, October 1966.

14. Monta, K., "Time Optimal Digital Computer Control of Nuclear Reactors, (III):- Experiment", J. Nucl. Sci. Technol., 4(2), 51, February 1967.

15. Harrer, J.M., "Nuclear Reactor Control Engineering", D. van Nostrand Co., Princeton, 1963.

16. Glasstone, S., "Principles of Nuclear Reactor Engineering", D. van Nostrand Co., Princeton, 1955.

17. Ash, M., "Nuclear Reactor Kinetics", McGraw-Hill Book Co., New York, 1965.

18. Rosztoczy, Z.R., "Optimization Studies in Nuclear Engineering", Ph.D. Thesis, The University of Arizona, Univ. Microfilms, No. 64-10, 458, 1964.

19. Woodcock, G.R., Babb, A.L., "Optimal Reactor Shutdown Programs for Control of Xenon Poisoning", Trans. Am. Nucl. Soc., 8, 235, 1965.

20. Rosztoczy, Z.R., Weaver, L.E., "Optimum Reactor Shutdown Program for Minimum Xenon Buildup", Nucl. Sci. Eng., 20, 318, 1964.

21. PDP-9 Users Handbook, Digital Equipment Corporation, Manyard, Massachusetts.

22. EAI - 231R Analog Computer Console, Electronic Associates Inc., Long Branch, New Jersey.

23. Marston, G.P., "Design of Medium Scale Hybrid Interface", M.A.Sc. Thesis, University of British Columbia, 1967.

24. Crawley, B., "Software for Medium-Scale Hybrid Computer", M.A.Sc. Thesis, University of British Columbia, 1969.

25. PDP-9 Macro 9 Assembler Manual, Digital Equipment Corporation, Manyard, Massachusetts.

26. Hastings, C., "Approximations for Digital Computers", Princeton University Press, 1955.

27. Instruction Manual for Linear Logarithmic Monitor Sperry Gyroscope Division, Sperry Rand Canada Ltd., Montreal.

28. Beckey, G.A., Karplus, W.J., "Hybrid Computation", John Wiley and Sons, Inc., New York, 1968.